PalZ
https://doi.org/10.1007/s12542-021-00599-y

RESEARCH PAPER

The discovery of widespread agrichnia traces in Devonian black shales of North America: another chapter in the evolving understanding of a "not so anoxic" ancient sea

Ryan D. Wilson[1,2] · Juergen Schieber[1] · Cameron J. Stewart[1]

Received: 22 April 2021 / Accepted: 22 November 2021

Abstract
For earth scientists, to examine how life forms interact with their environment is of key importance to understand evolutionary linkages and adaptations within the biosphere. The Devonian Period experienced many changes of marine and terrestrial ecosystems, most notably the proliferation of vascular plants that accelerated terrestrial weathering and nutrient flux to the oceans and resulted in globally extensive deposition of organic-matter-rich mudstones. In geologic history, such strata appear to be linked to global rise of sea level, greenhouse climate with elevated atmospheric pCO_2, active volcanism, and extinction events. A concerted effort in multiple fields is aimed at understanding the history of oxidation states, modes of organic-matter preservation, and how paleoredox conditions are influenced by local and global drivers (e.g., sea level, tectonics, volcanism). In this study, we document the discovery and unique preservational style of agrichnia (graphoglyptid) traces in Middle–Late Devonian organic-rich shales from three different basins across North America. On slabbed core surfaces the remains of these burrows appear as inconspicuous discontinuous, bedding parallel pyritic streaks, but X-ray computed tomography (CT) scans show bedding parallel pyritized polygonal structures that are interpreted as graphoglyptid burrows. Agrichnia are generally attributed to trace-makers capable of constructing interlaced branching structures to harvest microbial consortia in oxygen-stressed settings, and their discovery in black shales provides new perspectives for interpreting the benthic habitability of organic-rich depositional settings.

Keywords Agrichnia · *Paleodictyon* · Bioturbation · Black shales · Devonian

Introduction

Although organic-matter-rich, fine-grained sediments occur throughout earth history, there are discrete time intervals where they are of particular abundance due to global sea-level rise, greenhouse climate with elevated atmospheric pCO_2, and spikes of global volcanism (Fischer 1981). The Middle–Late Devonian represents one of these critical time periods of global organic-matter accumulation, presumably caused by greenhouse conditions with 4–12 times present day pCO_2 levels (Berner 1990). In North America (i.e., Laurentia), these unique strata have long been studied for clues to ancient climates, past ocean conditions, mass extinctions, and the origin of source rocks. They include the Frasnian–Famennian mass extinction event, one of the five greatest biotic crises of the Phanerozoic (Sepkoski 1986; Scotese and McKerrow 1990; McGhee 1996; Hallam and Wignall 1997; House 2002).

Historically, ichnology has been an under-utilized tool for interpreting paleoenvironments in black shales, owing in part to the difficulty to determine bioturbation intensity and diversity in these black sediments. Contributing factors are (1) low or absent optical contrast between burrow fill and host rock, (2) high degree of compaction of originally very water-rich sediments, and (3) the widespread perception that black shale deposition mostly occurs beneath a pycnocline with anoxic to euxinic bottom waters that cannot sustain benthic metazoans (Ettensohn et al. 1988; Schieber 2003). Detailed petrographic and high-resolution geochemical

Handling Editor: Joachim Reitner.

✉ Ryan D. Wilson
RyanWilson@chevron.com

[1] Department of Geological Sciences, Indiana University, 1001 E. 10th Street, Bloomington, IN 47405, USA

[2] Present Address: Chevron Energy Technology Company, Houston, TX 77002, USA

Published online: 03 December 2021

studies have shown that whereas bottom waters commonly were oxygen limited, truly anoxic conditions must have been exceedingly rare (Schieber 2003; Wilson and Schieber 2017). Prior ichnologic studies of black shale have been used to infer relative pore and bottom water paleo-oxygen concentrations (Jordan 1985; Ekdale and Mason 1988; Savrda and Bottjer 1989; Savrda and Ozalas 1993; Boyer and Droser 2011), substrate consistency (Lobza and Schieber 1999); shale fabric origins (Cuomo and Rhoads 1987; Cuomo and Bartholomew 1991; Schieber 2003), depositional environment (Sageman et al. 2003; Trabucho-Alexandre et al. 2012); and reservoir quality (Wilson and Schieber 2016; Wilson et al. 2020).

In the appraisal of depositional environments and paleoclimate studies, understanding pore and bottom water paleo-oxygen concentrations is of particular importance as fluctuations may be linked to tectonic or climatic changes which may have implications for organic-matter preservation (Savrda and Bottjer 1991; Sageman et al. 2003; Trabucho-Alexandre et al. 2012). A common technique to study burrow structures in modern sediments and drill cores involves 3D reconstructions (Savrda et al. 1984; Savrda and Ozalas 1993; Schieber 2002; Wetzel 2010; Bednarz and McIlroy 2012), an approach that is greatly aided by the recent introduction of X-ray computed tomography (CT; Ketcham and Carlson 2001; Mees et al. 2003). An advantage to this methodology is the non-destructive approach, and that through software-aided segmentation, 3D models of specific burrows can be generated.

This study of three Middle–Late Devonian organic-matter-rich shale successions from across North America documents a unique pyritic preservation style of agrichnia traces. These are the first of its kind identified in the Devonian time period or any deep-time black shale succession for that matter, and represent a significant advance in understanding benthic redox conditions during an important time period in Earth history.

Geologic setting

Samples from three different locales and Devonian time intervals were investigated for this study (Fig. 1), the Givetian Geneseo Shale of the northern Appalachian Basin (New York), the Givetian–Famennian New Albany Shale of the Illinois Basin (Indiana), and the Famennian–Tournaisian Bakken Shale of the Williston Basin, North Dakota (Fig. 2). Of these, the Geneseo Shale represents the most proximal setting relative to the Acadian Fold Belt (Fig. 2), deposited in a retroarc foreland basin that was the primary depocenter for siliciclastics shed from the Acadian Orogeny (Ettensohn et al. 1988; Faill 1985). During Geneseo deposition, the northern Appalachian Basin was located approximately 30°−35° south of the equator (Witzke and Heckel 1988; Fig. 2). Environmental conditions were seasonally variable and ranged from arid to semi-arid (Witzke and Heckel 1988; Woodrow 1985). A mental image of continental flooding associated with limited water circulation has long been a key factor in many depositional models for Devonian organic-matter-rich mudstones in the Appalachian basin (Algeo et al. 2007; Sageman et al. 2003; Werne et al. 2002). The lower Geneseo Shale of western New York shows aggradational to progradational parasequence stacking from east to west, with organic content (up to 8% total organic carbon, TOC) increasing westwards, away from clastic dilution (Wilson and Schieber 2017; Smith et al. 2019).

The Givetian–Famennian New Albany Shale occurs in outcrops and in the subsurface throughout much of the Illinois Basin (Lineback 1968, 1970; Schieber and Lazar 2004), a feature that began as a rift complex and evolved into a cratonic embayment during the Paleozoic Era (Buschbach and Kolata 1991; Kolata and Nelson 1990). Relative to the Geneseo Shale, the New Albany Shale was deposited more distal to the Acadian Fold Belt, separated from the Appalachian Basin by a structural high, the Cincinnati Arch (Fig. 2). Due to this distance, shale facies in the New Albany are generally finer grained, and due to reduced clastic dilution show TOC in excess of 20 wt.%.

The Famennian–Tournaisian Bakken Shale was deposited in the intracratonic Williston Basin that extends in the subsurface from Saskatchewan to Montana and the Dakotas. Its three subdivisions (Fig. 1) unconformably overlie the Late Devonian Three Forks Formation and conformably underlie the Mississippian Lodgepole Formation, and are interpreted to have been deposited in an open-marine shelf environment (Montgomery 1996). Of our three examples, the Bakken was deposited most distal to the Acadian clastic source to the east (Fig. 2), and shows organic enrichment in excess of 20 wt.% TOC.

Methods

The present study is based on observations from 19 drill cores that span the northern Appalachian Basin (4), the Illinois Basin (12), and the Williston Basin (3). Observations concerning lithology, facies, texture, and diagenetic overprint were made mostly on slabbed cores and petrographic thin sections. Cores and core samples were scanned or photographed for collection of digital images that could be processed for feature enhancement. The basic procedures for core description were those outlined by Lazar et al. (2015a, b).

X-ray computed tomography (CT scanning) involves producing tomographic slices/images from computer-processed X-rays that can be used to create 3D images of the

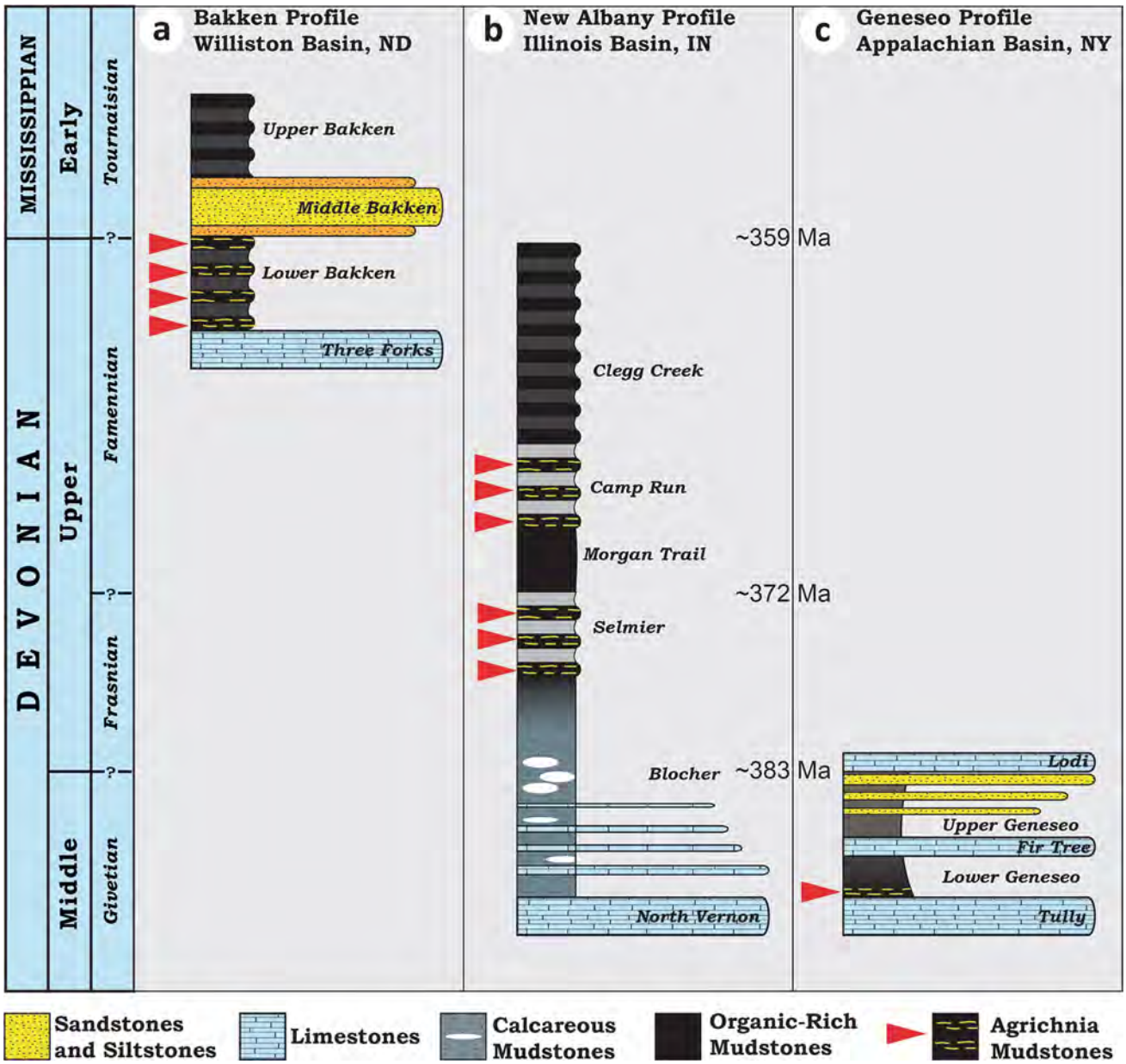

Fig. 1 Stratigraphic context of the three Devonian black shale successions examined for this study. **a** Bakken Shale, **b** New Albany Shale, **c** Geneseo Shale. Red arrows show stratigraphic position of agrichnia bearing black shales

X-rayed volumes (Ketcham and Carlson 2001; Mees et al. 2003). The CT scans were used to: (1) better visualize the 3D form of burrows in the New Albany Shale, (2) identify burrows difficult to observe on the basis of slabbed core surfaces (e.g., pyritic trails, obliquely cut traces, and traces "hidden" in the rock volume), and (3) understand their abundance, pervasiveness, and interrelationships. CT scan data were viewed and analyzed using 3D CorView software provided by Weatherford Labs. Samples of pyritic traces were argon ion-milled for scanning electron microscopic (SEM) examination following procedures outlined by Schieber (2013), and Schieber et al. (2016). X-radiographs of New Albany Shale samples were made at an industrial lab for welding inspections.

Prelude–enigmatic bioturbation in the New Albany Shale of Indiana

Looking for subtle hints of bioturbation has been an enduring thread in studies of black shales and is an ongoing pursuit (Schieber et al. 2021, Schieber and Wilson 2021, this

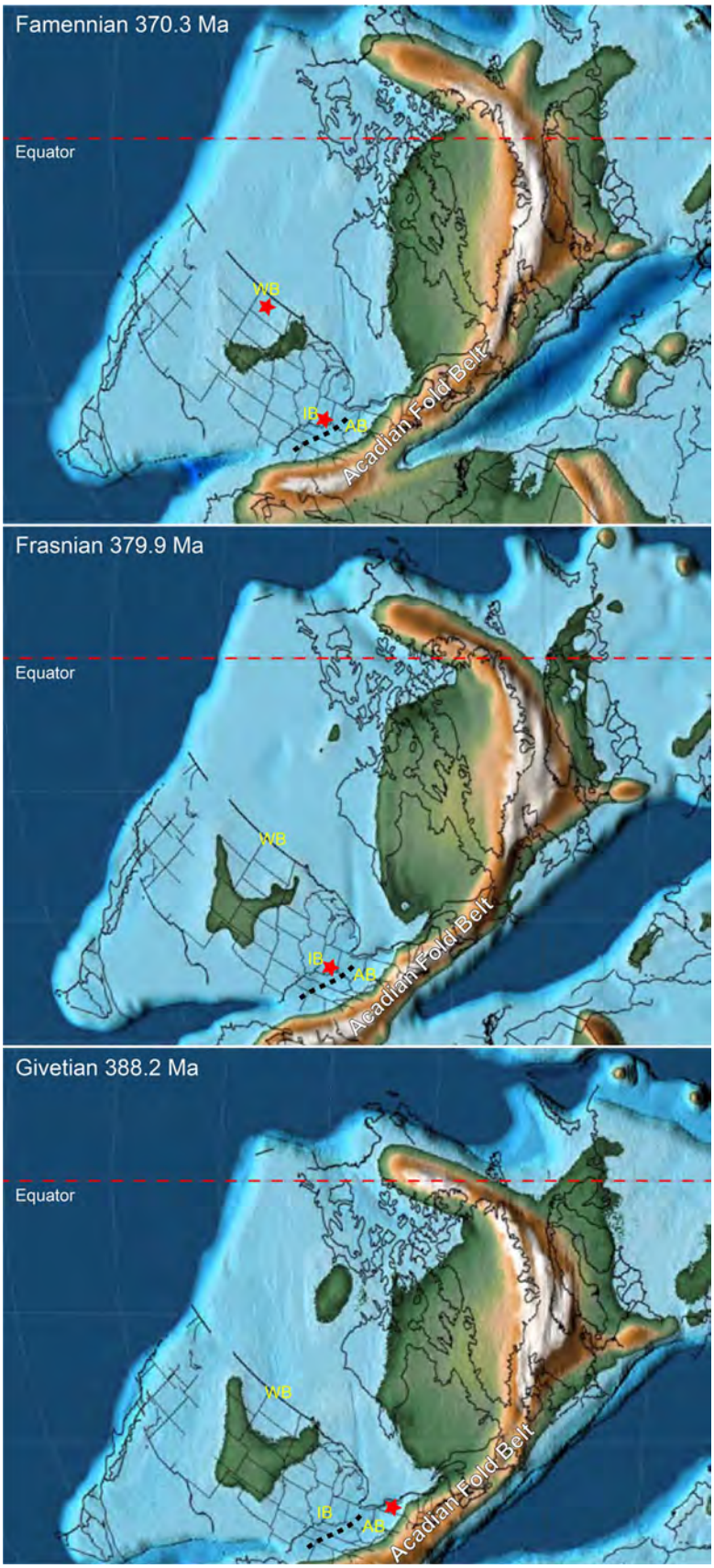

Fig. 2 Paleogeographic context of the three study areas (red stars). *AB* Appalachian Basin; *IB* Illinois Basin; *WB* Williston Basin. Black dashed line Cincinnati Arch. Time slices from Scotese, 2014

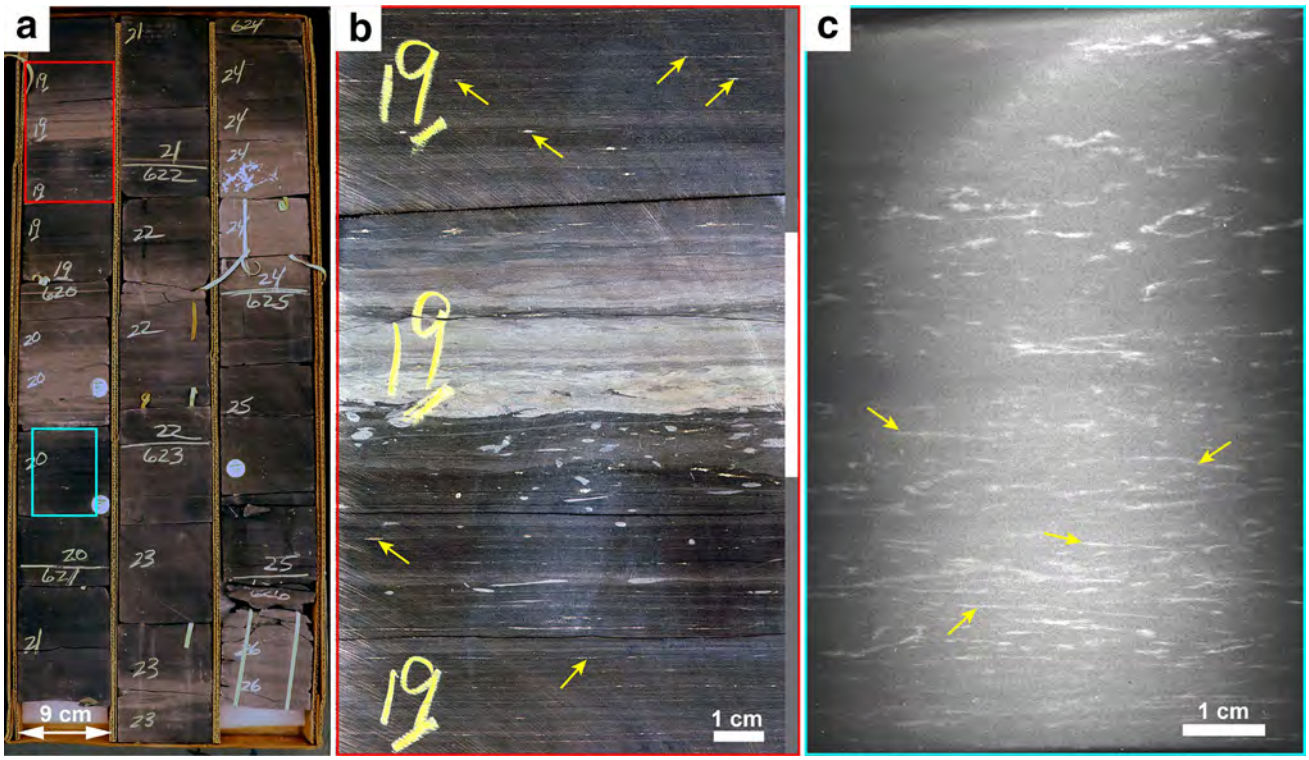

Fig. 3 **a** A box of drill core from the New Albany Shale of Indiana, USA. Shows light colored bioturbated intervals that alternate with laminated black shale. **b** A detailed view of the area marked with a red frame in a, that shows a light colored bioturbated interval over a darker laminated interval (red dashed line marks the boundary). Yellow arrows point to silt/pyritic streaks. **c** X-radiograph of black laminated interval marked with blue frame in a. Yellow arrows point to low-angle inclined dense linear features that are presumed to be pyritic

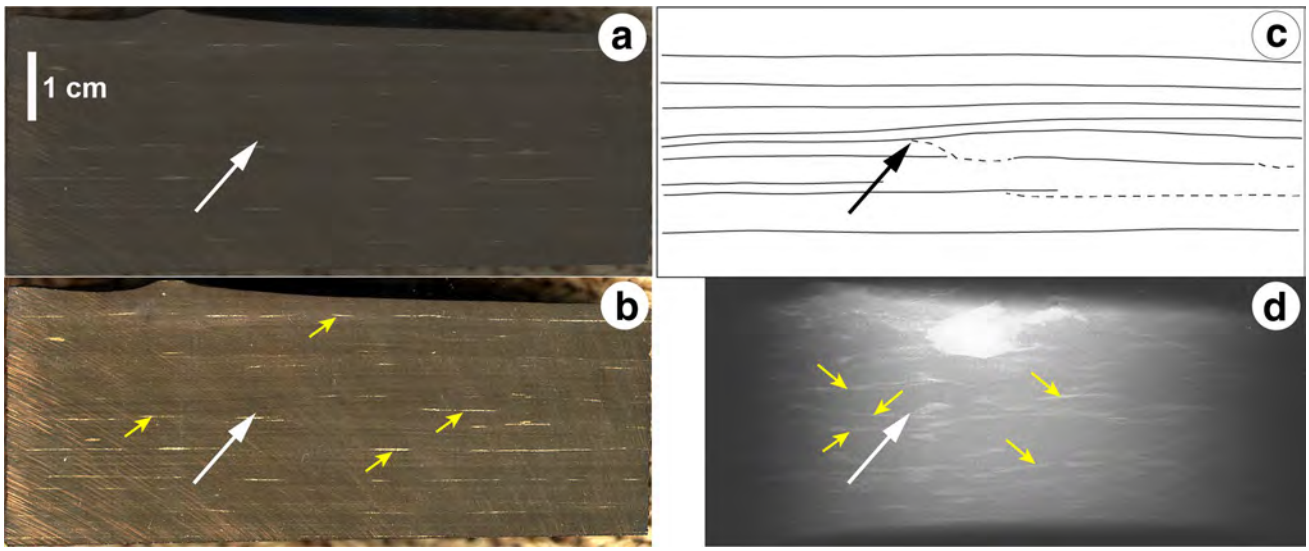

Fig. 4 Images of a specimen of "silt-streaked" black shale. **a** An image of a smoothed core sample. The scale bar applies to all other portions of the figure. **b** Same image, but contrast enhanced. Yellow arrows point to bright streaks of pyrite. **c** A sketch of lamina irregularity and lamina truncations. The black arrow points to a truncation, and is replicated in white in the other frames. **d** An X-radiograph of the same sample. Yellow arrows point to low-angle inclined dense linear features that are presumed to be pyritic. The left edge is not shown because it was completely over-exposed (drill core samples thin towards the edge). There is a pyrite nodule (white blob) in the top of the sample that is not exposed on the surface

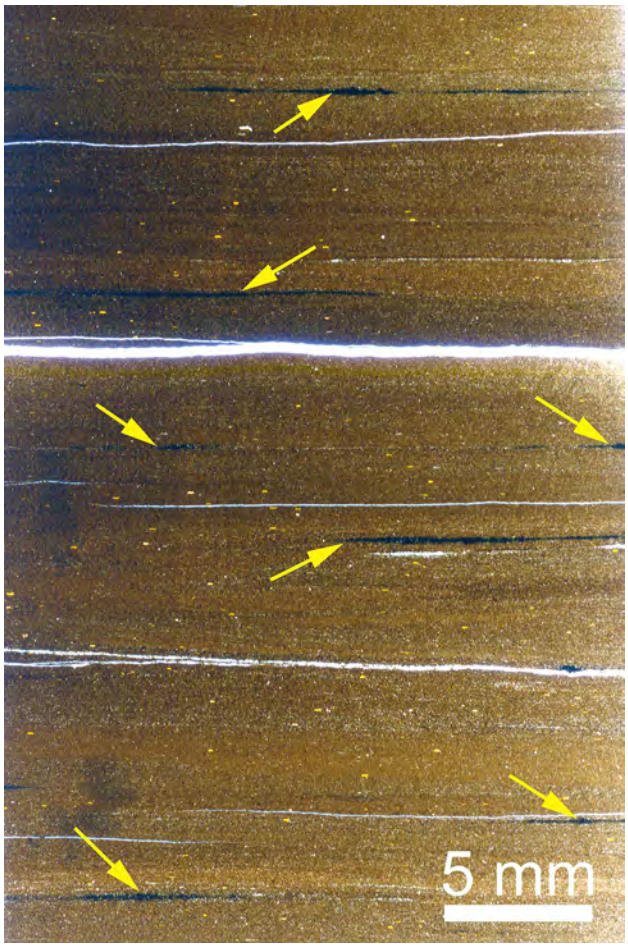

Fig. 5 Transmitted light images are shown, thin section scan of "silt-streaked black shale" that shows pyritic streaks (yellow arrows). They are opaque in transmitted light, but will appear bright in reflected light. Note that there is little in terms of primary lamination. There is a horizontal fabric, but it consists of compositional bands that are probably the result of meioturbation (Schieber and Wilson 2021, this volume)

issue). In an earlier study (Schieber 2003), a specific facies of black shale was encountered within the Camp Run member of the New Albany Shale (Schieber and Lazar 2004) that occurs interbedded with visibly bioturbated intervals (Fig. 3a). When looked at more closely, the black shales have a laminated character (Fig. 3b) of the kind that one may see in many other laminated black shales in the rock record (O'Brien and Slatt 1990). These black shales showed discontinuous streaks of silt, and led to the term "silt-streaked black shales" when describing these rocks in drill core. What was puzzling though was that these streaks of silt (Fig. 3b) were slightly non-parallel and showed variable orientation across the specimen surface (Fig. 4). Closer inspection showed that the streaks were actually pyritic rather than silty (Fig. 5). X-radiographs prepared from these samples, with samples oriented so that bedding planes were approximately perpendicular to the X-ray film, showed an interesting difference between the cut surface and the internal fabric as seen in X-ray images. Whereas the black shale layers look outwardly parallel laminated with light pyritic lenses or streaks (Fig. 3b), internally (X-radiographs) we see linear dense features (pyritic) that are oriented at a low angle to the horizontal plane (Fig. 3c). This is not what one intuitively expects if these streaks or lenses were something produced by bottom current activity that leads to sediment reworking and concentration of denser particles. Figure 6 illustrates the difference between physically produced laminae and the low-angle linear features within the "pyrite-streaked" shales. What was also notable was the fact that in contrast enhanced images (Fig. 4b, c) subtle discontinuities and lamina disruptions became visible. A key focus was determining if these features were a product of bottom current reworking or of biologic origin. In drill cores lateral tracing of discontinuities and lamina disruptions is impeded because of small sample size, whereas in outcrop samples unloading fractures and even the slightest weathering serves to completely obscure them. Systematic core description, however, uncovered several specimens that established that the "pyrite-streaked black shales" must have been the product of bioturbation (Fig. 7).

Whereas the cross-cutting relationship between "pyrite-streaked" fabric and an earlier homogeneous fabric (Fig. 7) implies that the former is definitively post-depositional and most plausibly due to bioturbation, what kind of organism was responsible was not clear at this point. The burrowers seem to have moved through the sediment more or less horizontally, producing what one might call a burrow-laminated fabric. The homogenous fabric is likely a result of very early fabric reworking by meiofauna (Schieber and Wilson 2021, this issue) suggesting oxygen limited conditions at the seabed, yet also indicating an absence of anoxic bottom water conditions. The organisms that produced the pyrite-streaked fabric appear to have been larger than meiofaunal organisms, probably several mm in diameter. The latter estimate is based on the fact that the laterally terminating layer in Fig. 7 (green arrow) is 1 mm thick and has undergone severe compaction. A remarkably discrete macrobioturbator indeed.

In multiple X-radiographs, the pyritic streaks are confined to discrete horizons within the pyrite-streaked material, and also exhibit narrow angle junctions between pyritic linear features (Fig. 8). In some X-radiographs these horizons appear rather thin (Fig. 8a), in others they are a bit thicker. When first examining these X-radiographs in 1999, the assumption was that pyritic streaks occurred on a somewhat undulous plane or surface, and that the interwoven or lattice-like appearance of streak horizons (Fig. 6) was brought about by seeing the streaks "side on" because the imaging axis (X-ray beam axis) was parallel to these surfaces. This was still the preferred interpretation in Schieber

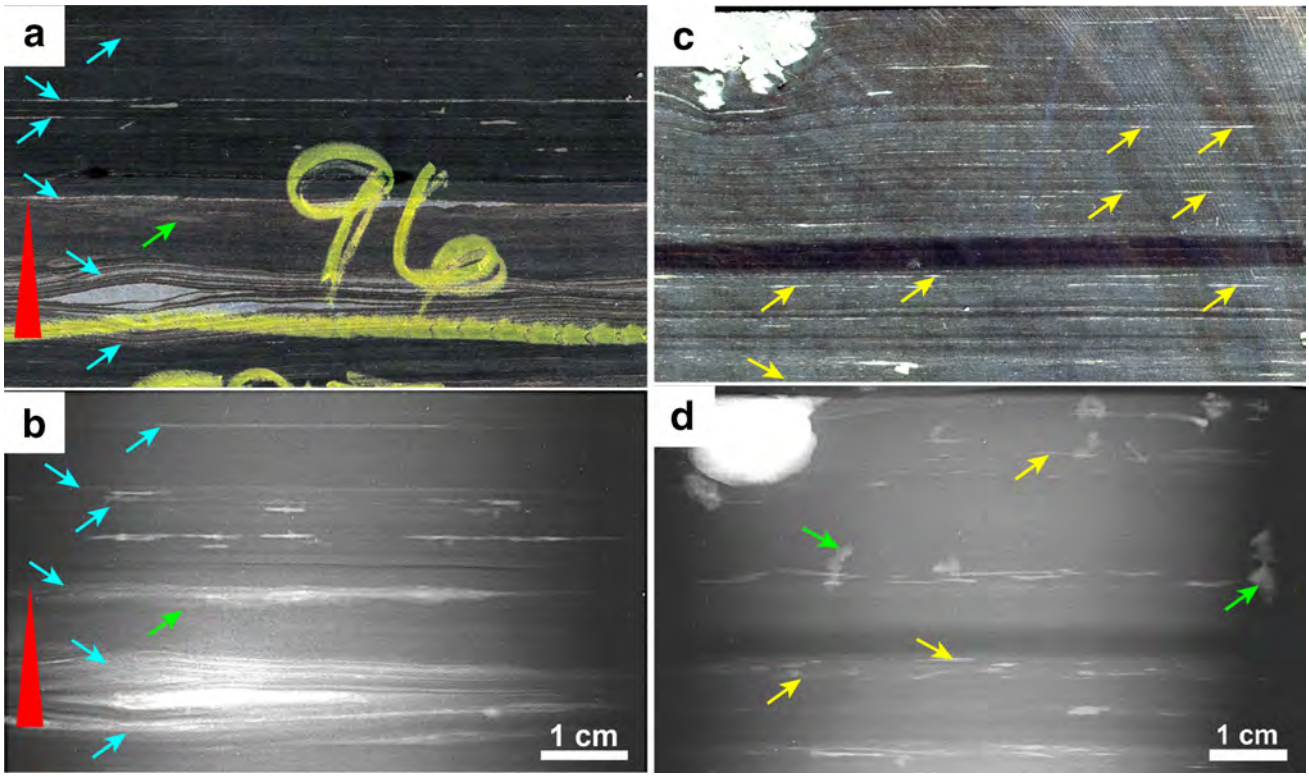

Fig. 6 A comparison between the core slab and X-radiograph appearance of true physical laminae (**a**, **b**) and the laminae as seen in "silt-streaked black shale" (**c**, **d**). **a** Contrast enhanced image shows a graded bed with silt ripple lamination in the base (red wedge), and continuous silt laminae are marked with blue arrows. Bioturbation in the top of the graded (event) bed is marked with a green arrow. **b** An X-radiograph of the same sample. Physical laminae are flat and continuous and marked with blue arrows. The bioturbation from a (green arrow) does not show because density contrast is too low. **c** Contrast enhanced image of "silt-streaked black shale" with pyritic streaks marked by yellow arrows. **d** The complementary X-radiograph that shows low-angle inclined dense linear features that are presumed to be pyritic (yellow arrows), as well as subvertical pyritic features (green arrows) that are probably pyritized burrows (Schieber 2003)

(2003), owing to the fact that we had used our available tools (core description, thin sections, X-radiographs) to their fullest extent and could go no further. New ways to visualize these features were needed.

The tool that would move our understanding to a new level, X-ray computed tomography, as used with medical CT scanners, already existed, and had already been adapted to scanning of rocks by Shell and Terratek (an oil field services company in Salt Lake City, Utah) by the mid-1980s. It was initially used for characterization of oil reservoirs, and quite expensive. By the late 1990s the first shale cores were examined with CT scanners by Terratek, and in the 2000s a growing number of other oil field service companies started to offer CT scanning of drill core. With the onset of the "shale boom" in 2006, CT scanning of shales was increasingly applied for characterization of shale gas reservoirs. It still was expensive, though, for academic applications. However, because the IU Shale Research Lab (IUSRL) had extensive industry sponsored projects by that time, we were able to have a set of New Albany Shale cores CT scanned in 2012 (financed by Shell), and finally to see the "inside" of these rocks was an eye opener.

Results

Pyritic streak black shales in the New Albany Shale

Descriptions of New Albany Shale cores in the core library of the Indiana Geological Survey were scrutinized for occurrences of pyrite-streaked black shale, and promising examples from four cores were selected for CT scanning at Weatherford Labs in Houston, Texas. Pyrite-streaked black shale occurs in both the Frasnian Selmier Member and the Famennian Camp Run Member (Fig. 9) of the Late Devonian New Albany Shale (Schieber and Lazar 2004). Both shale members are characterized by decimeter–meter-thick laminated appearing black shale intervals that alternate with visibly bioturbated interlayers of gray shale (Fig. 10), and pyrite-streaked black shale is best and most extensively developed

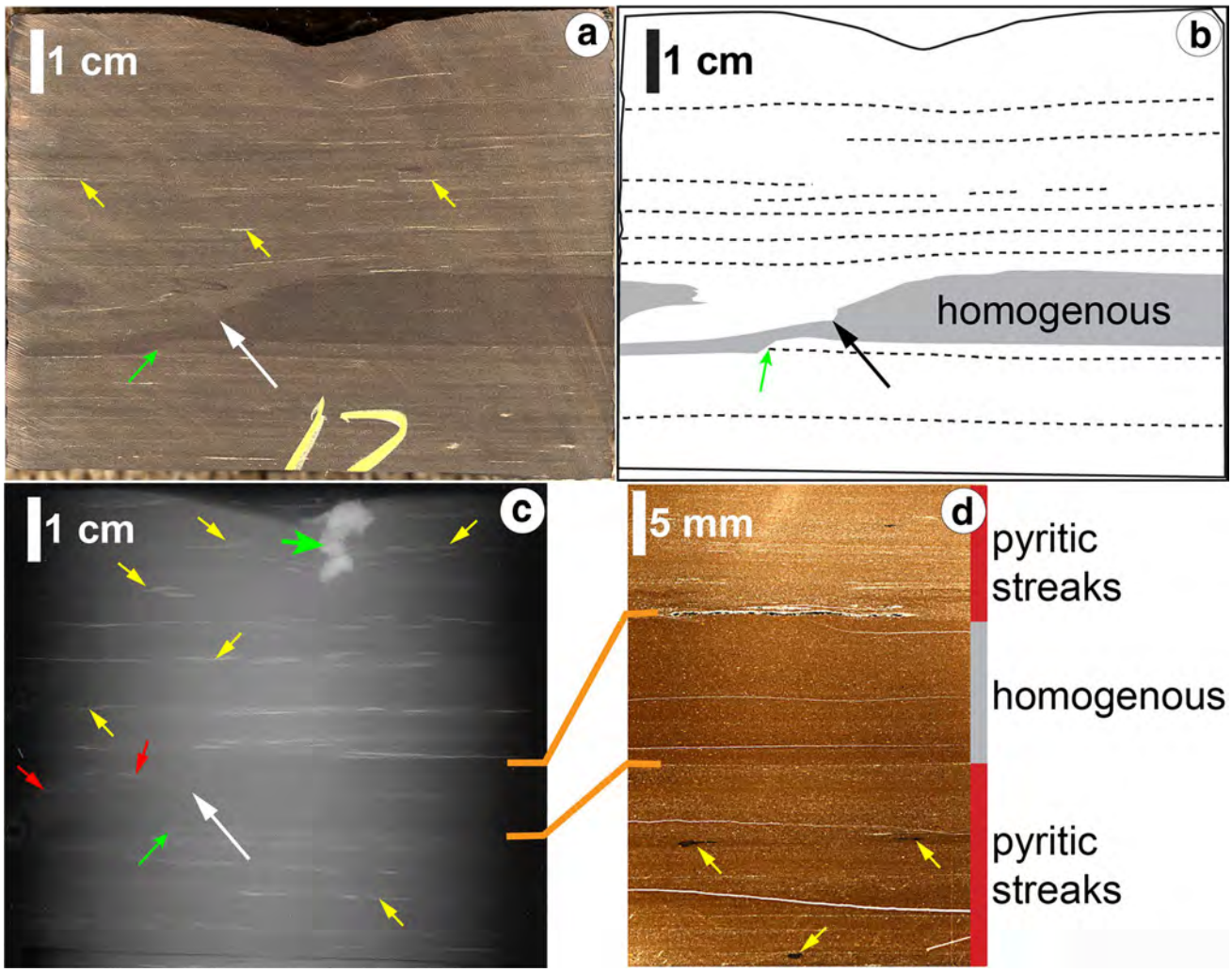

Fig. 7 A "lucky" sample of the "pyrite-streaked" black shale with traces shown in Figs. 1, 2, 3, and 4. **a** Core sample shows typical facies with pyritic streaks (yellow arrows), and a darker layer that lacks them (contrast enhanced image). The white arrow points to a place where the streaked facies cuts across the dark layer. A green arrow points to a place where one of the internal layers of streaked material terminates laterally. **b** A drawing of A that shows these relationships more clearly. **c** An X-radiograph of the sample shown in a, the white arrow is identical in position the white arrow in a. The contrast between the darker interlayer (homogenous) and the pyrite-streaked material is minimal, but pyritic streaks are visible in the cross-cutting portion (red arrows). Green arrow points to laterally terminating layer. Bold green arrow points to a pyritized burrow. **d** A thin section of part of the sample that captures the darker homogenous appearing layer and adjacent pyritic streak material

in the black shale intervals of the Camp Run Member. The horizontal fabric of the black intervals shows compositional banding (Fig. 5) suggestive of meiofaunal reworking (Cullen 1973; Pike et al. 2001, Cuomo and Rhoads 1987) of the surface sediment (Schieber and Wilson 2021, special issue), as well as lamination developed due to horizontal movement of a "mystery" trace maker (Fig. 7).

In New Albany cores that were CT scanned, bedding parallel irregular polygonal structures were observed in all cores, and are generally more abundant in the Camp Run Member than the Selmier Member. Although polygonal structures occur in both black and gray (macrobioturbated) intervals (Fig. 8), they are much more abundant in intervals that are not visibly macrobioturbated. From the CT scans, it appears that polygonal structures in gray intervals are cross-cut by macro-burrows (e.g., *Zoophycos*) and as such have lower preservation potential. The polygonal structures appear as bright features on CT scans, owing to association with diagenetic pyrite that was observed on cut surfaces (Fig. 4) and in thin sections (Fig. 5). The dimensions of

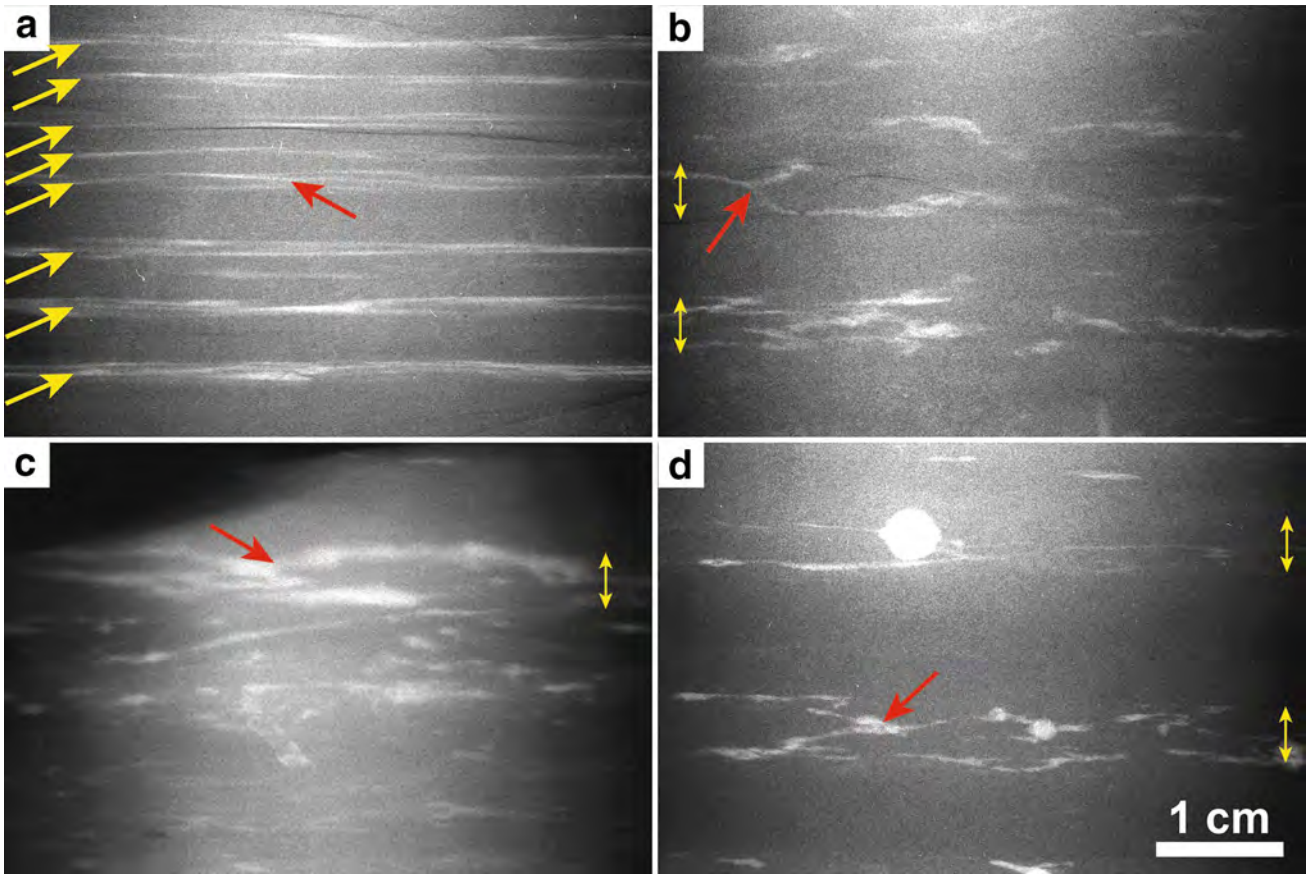

Fig. 8 Variable appearance of pyrite-streaked horizons in X-radiographs. The scale is the same for all images. **a** Comparably thin pyrite-streaked horizons (yellow arrows) with low-angle inclination (to the horizontal) of individual streaks. Red arrows in all images point to narrow angle junctions between streaks. **b**, **c**, **d** Thicker streaked horizons, yellow double arrows indicate presumed thickness of horizon

polygons vary between cores and core intervals, but generally measure 1–2 cm across. Textural examination by thin section petrography and SEM shows that pyritic polygon traces are oval in outline, suggesting an original round-cylindrical shape that was flattened due to compaction of the water-rich original mud. Within the pyritic traces, mineral inclusions appear to "float" within the pyrite, indicating sediment-inclusive growth in a very water-rich matrix (Fig. 11). The wide particle separations in Fig. 11a actually suggest suspension of the particles in an organic slime matrix (Schieber 2002), consistent with a worm burrow in a water-rich substrate.

Pyritic streak black shales in the Bakken Shale

A few years after the opportunity to look "inside" the New Albany Shale with CT scans, another sponsor of the IUSRL (Whiting Oil) made available a drill core with a set of CT scans from the Devonian–Mississippian Bakken Shale of the Williston Basin in North Dakota. The lower portion of the Bakken Shale is of Famennian age (Fig. 1) and showed the same pyritic streak black shales as already observed in the New Albany Shale (Fig. 12a). The pyritic streak horizons in CT scan view are spaced as closely as a few millimeters (Fig. 12b), which in terms of the original uncompacted sediment (assuming 85 vol% water content) suggests that these polygonal structures were originally stacked as close as 5 mm and as far as several centimeters apart. Polygon visibility is a matter of pyrite concentration, and whereas the planar polygonal structures are unmistakable when the movie clips of CT scan progression are viewed, the structures in any specific plane are less "complete" (Fig. 12c, d) when compared to those observed in the New Albany Shale (Fig. 10). The pyrite appears to be more concentrated in the corners of polygons, and less abundant in the sides (Fig. 12c). The polygon horizon as illustrated in Fig. 12

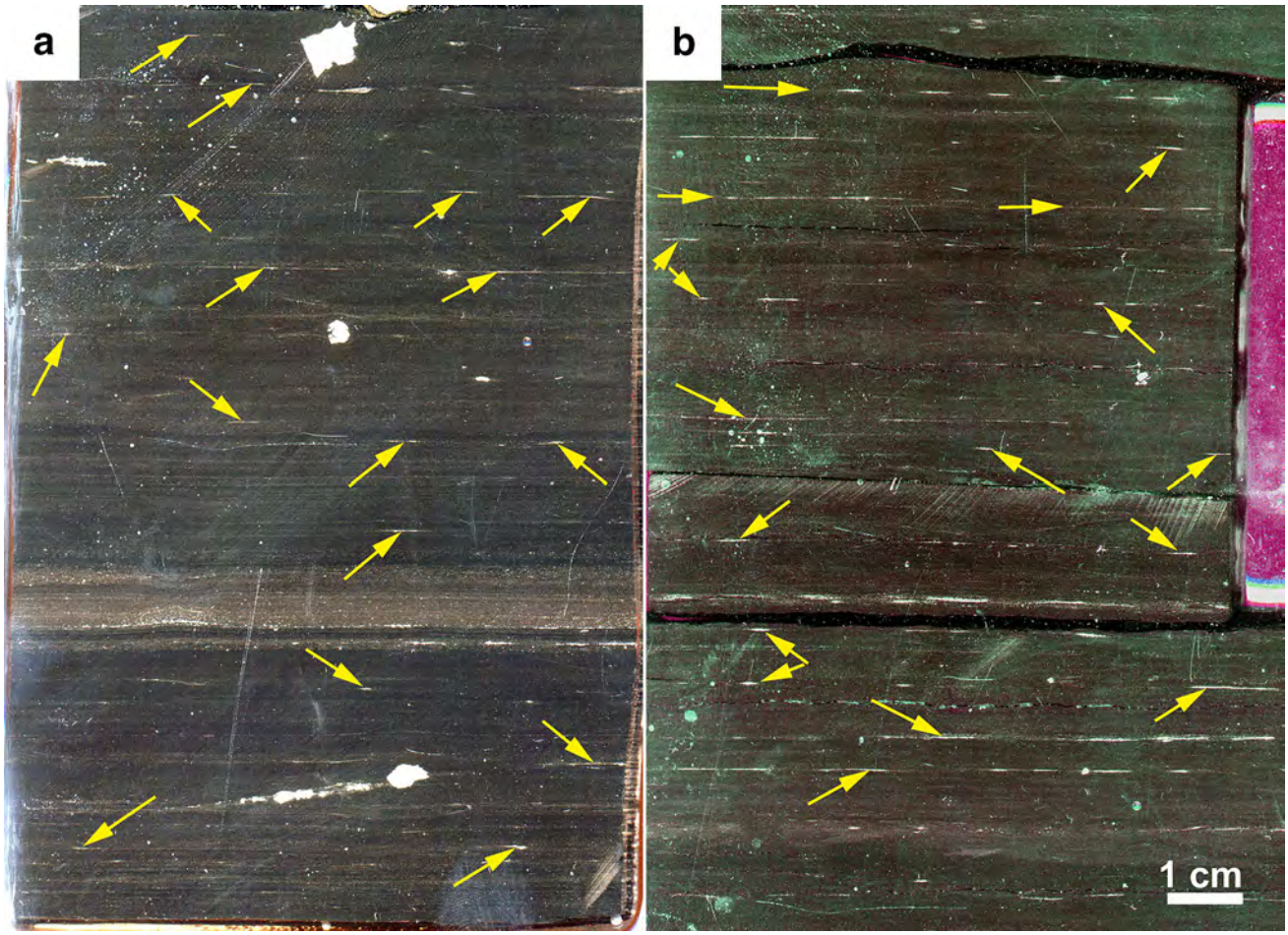

Fig. 9 Contrast enhanced "pyrite-streaked black shale" in the Selmier (**a**) and Camp Run Members (**b**) of the New Albany Shale. In both members this facies has the appearance of being laminated, but laminae may be due to horizontal movement of burrowing organisms (Fig. 6). Yellow arrows point to pyritic streaks

is typical for the Lower Bakken in this core. Unlike in the New Albany Shale (Fig. 10), there are no gray-colored bioturbated horizons interspersed with pyrite-streaked black shales. Instead, the pyrite-streaked black shales with polygon horizons contain 5–20 cm thick intervals that, while still black, are dominated by subhorizontal pyritic traces (Fig. 13). These intervals are associated with higher rock density (less organic matter, lighter color of core in CT scan). The original subvertical orientation suggests an affinity to *Skolithos* type trace fossils, although we are aware that *Skolithos* typically is found in sandy facies.

Pyritic streak black shales in the Geneseo Shale: a key indicator for polygon horizons

The oldest black shale interval examined for this study is the Givetian age Geneseo Shale of New York (De Witt and Colton 1978). For this example, we have images from slabbed cores, X-radiography, X-ray fluorescence, hand samples, thin sections, and SEM images (Figs. 14, 15, 16). The rocks have the same "pyrite-streaked" appearance as those described from the New Albany and Bakken shales, as well as similar compositional variance (Fig. 16) and pyrite textures (Fig. 14). From our observations, the similarity in facies is so striking that we predict that once CT scans have been acquired, pyritic polygons as observed in the New Albany Shale and the Lower Bakken Shale will be confirmed. In the Geneseo Shale, the basal contact with the underlying Tully Limestone (Figs. 1, 16) constitutes a westward progressing onlap (Taghanic Onlap) onto a structural high (Cincinnati Arch) that forms the western margin of the Appalachian Basin (Smith et al. 2019). The lowermost Geneseo black shales represent an extremely condensed stratigraphic section enriched in TOC and redox-sensitive trace metals (Fig. 16) with very small net sedimentation rates where pyritic facies are abundantly observed.

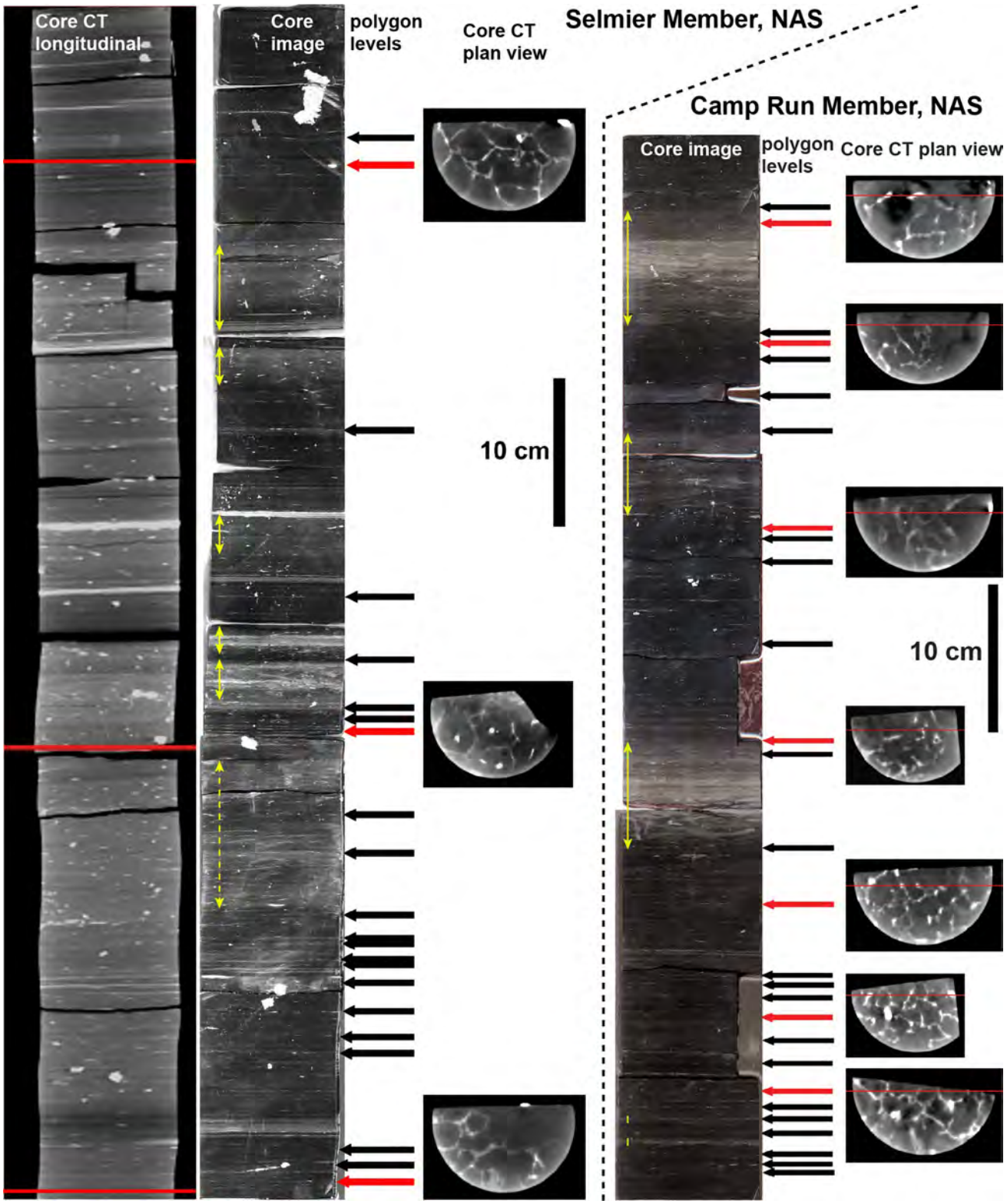

Fig. 10 Alternating macro-burrowed intervals (yellow double arrows) and pyrite-streaked black shale in the Selmier (left) and Camp Run Members of the New Albany Shale (NAS). The black arrows point to location of pyritic polygons. The red arrows are locations of polygons associated with a plan view image of the layer

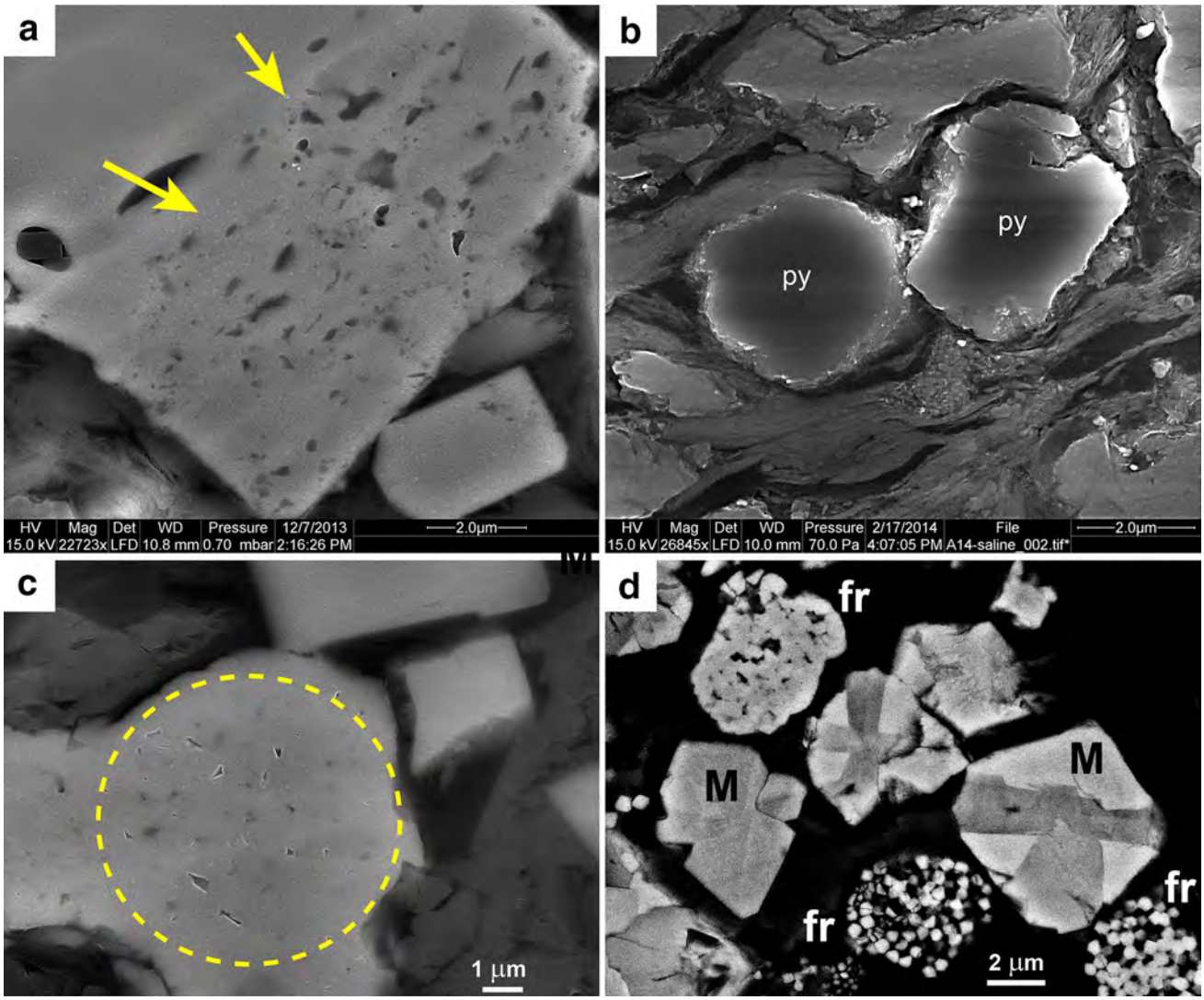

Fig. 11 Details of pyrite texture. **a** Pyrite from polygon cross section with abundant mineral inclusions (yellow arrows). The inclusions are widely separated, suggestive of "suspension" in an organic slime matrix that was subsequently pyritized (Schieber, 2002). **b** Pyrite grains (py) in the rock matrix that are not associated with polygons. These are free of inclusions and probably formed in pore spaces of the original water-rich mud. **c** The pyrite that composes the polygon cross sections also contains heavily cemented and overgrown framboidal pyrite (yellow dashed circle). **d** Some of the euhedral Fe-sulfide grains are actually twinned marcasite grains (Schieber 2011a, b)

Discussion

Implications for agrichnia traces in presumed anoxic shales

Given that the polygonal structures observed in the New Albany and Bakken Shales are preserved by means of early diagenetic pyrite, and given that the facies that contains them cuts across pre-existing shale fabrics (Fig. 7), it appears inescapable that the polygons formed post-depositionally in a water-rich substrate. The following observations support a biogenic interpretation for the polygons: (1) Their decompacted cross section shows resemblance to the body form of an organism; (2) They show dimensional continuity; (3) They show a regular and complex geometric pattern; (4) They are uniform in size (Figs. 10, 12); (5) They are preserved in full relief (Fig. 12); and (6) show possible burrow linings (Fig. 12). Burrowing marine worms, such as polychaetes, are often tubular in shape, and their resulting burrows are therefore cylindrical in form. Burrows found in black shales, however, are commonly oval or compressed vertically due to the high initial water content of these sediments (Jordan 1985; Lobza and Schieber 1999; Schieber 2011a).

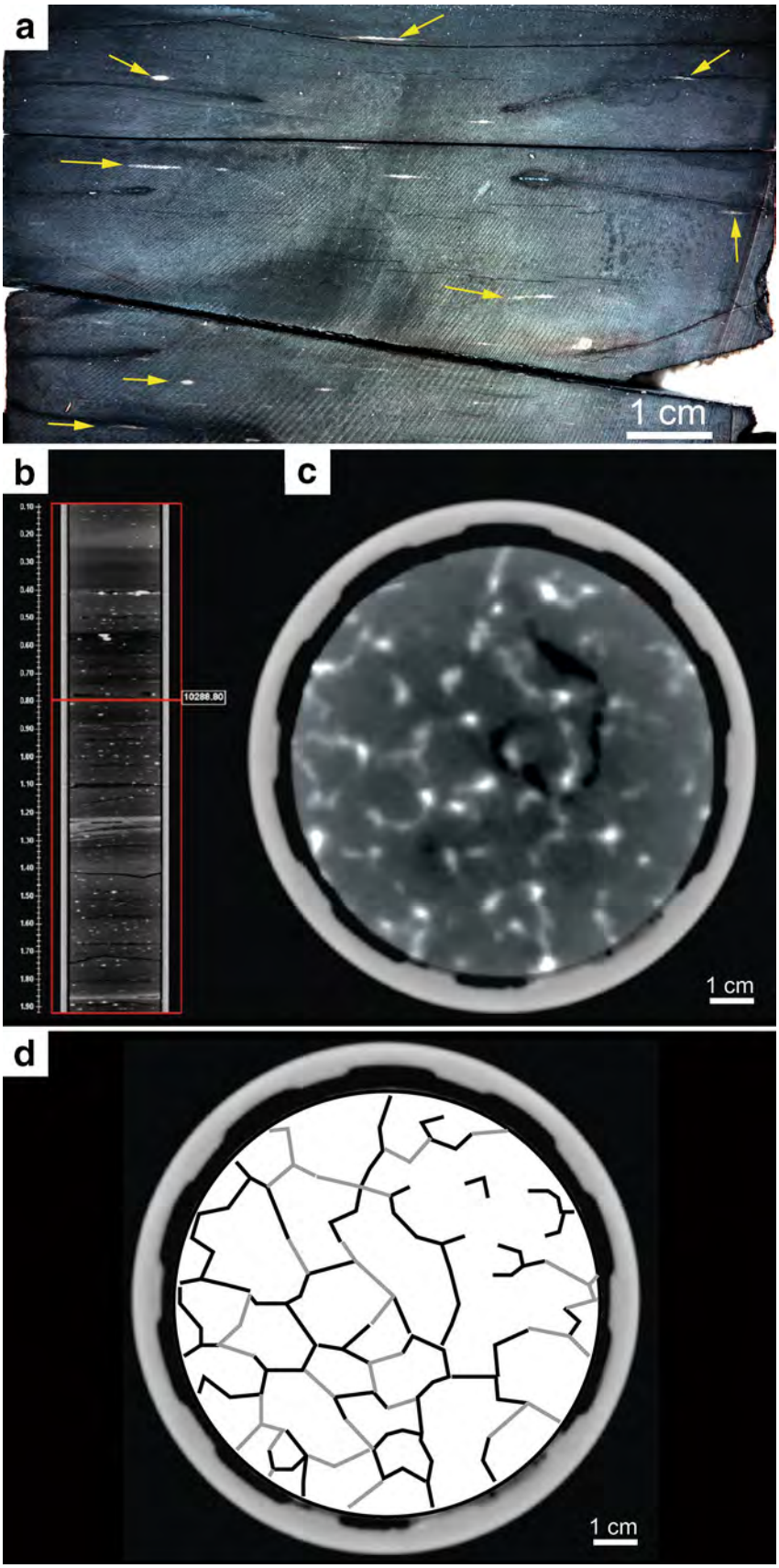

Fig. 12 **a** Photo of Lower Bakken drill core with thin streaks of pyrite (yellow arrows) in a black shale matrix. **b** Longitudinal CT scan of a core section (~ 60 cm long) with abundant polygon horizons. Pyritic streaks related to polygons are seen as oval bright spots (*py* pyrite). **c** Horizontal CT scan slice that shows polygonal pattern from the are in the core that is marked with a horizontal red line in (**b**). **d** A sketch of the polygons from (**c**), where the readily visible portions are marked with black lines, and faintly visible and extrapolated portions are shown with gray lines (*fr* pyrite framboid, *M* Marcasite)

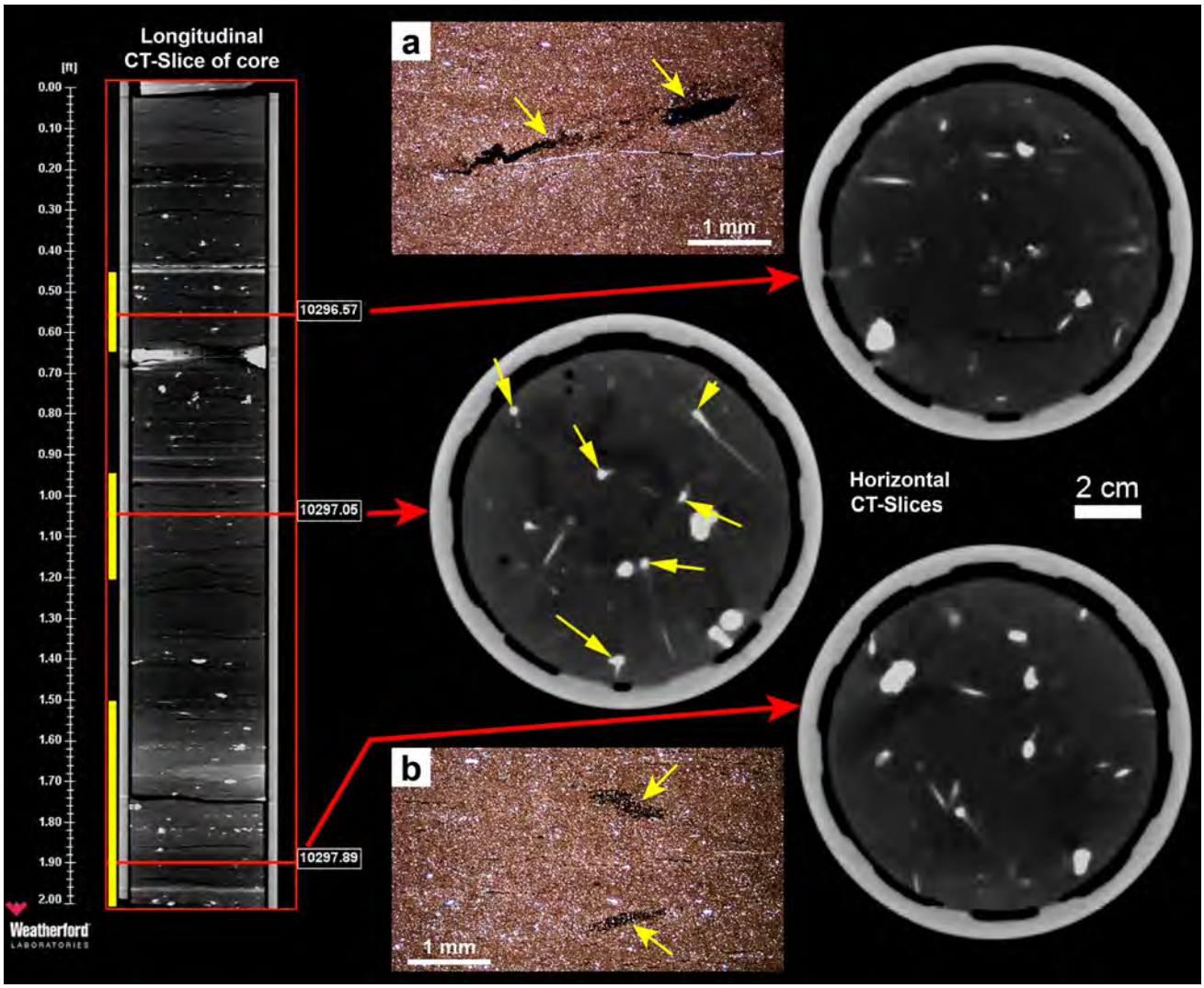

Fig. 13 At left the longitudinal CT scan image of a piece of Lower Bakken core of 60 cm length. Yellow bars to the left of the core image mark intervals that are dominated by subhorizontal pyritic traces, the remainder of the core is dominated by pyritic polygon horizons as seen in Fig. 12. At right, three examples of horizontal CT slices. They look rather different from the horizontal slice with polygons in Fig. 12. Yellow arrows point to the intercept of subhorizontal traces with the scan plane. Note associated bright "tails", which appear to be due to continuations of these traces to depth. Images a and b are thin section photomicrographs (perpendicular to bedding) that show intercepts of subhorizontal pyritic traces (yellow arrows)

The incompleteness of given polygons in CT scans is likely due to the fact that their detection hinges on the presence of pyrite, because macro-burrows that visibly destroy sediment fabric are rather inconspicuous or even invisible in X-radiographs due to a lack of density contrast. Diagenetic pyrite formation requires availability of reactive iron, and iron availability (from coatings on detrital grains) is linked to terrestrial weathering. An additional source of iron which also should also be accounted for is diagenetic recycling (Raiswell and Canfield 1998). From that perspective, the observation that Bakken polygons (Fig. 12) are generally less complete than New Albany polygons (Fig. 10), is consistent with a greater distance to the detrital source in the east (Fig. 2). Other mechanisms that could cause localized pyrite precipitation along polygons include: (1) the presence of mucus linings along the burrow margins, or (2) fecal pellets within or along the margins of the structure. In both cases the associated organic matter could be a food source for sulfate reducing microbes (Brett and Allison 1998). However, given that the polygons are surrounded by abundant matter, organic matter in itself is unlikely to act as a focal mechanism for pyrite formation.

The apparent compaction of the polygon tunnels suggests formation in a very water-rich substrate close to the sediment water interface (e.g., Schieber 2011a), in agreement with studies of modern sedimentary pyrite formation that

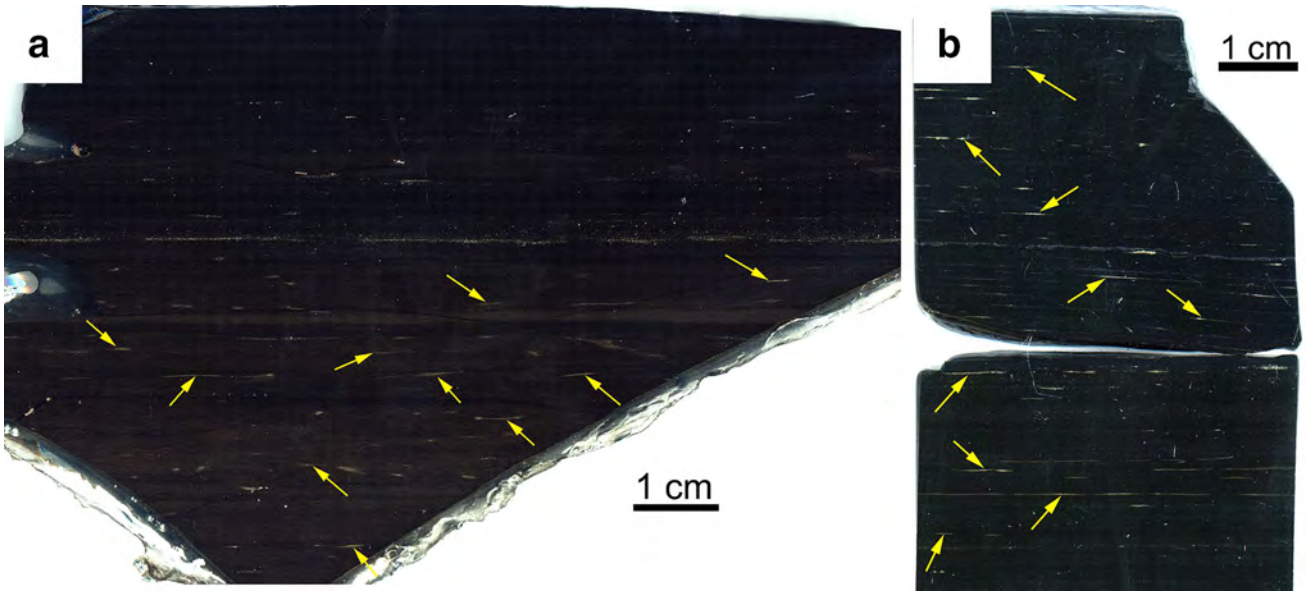

Fig. 14 Two examples of pyritic streak black shale from the Geneseo Shale. Both samples are from the western part of New York state, where the Geneseo onlaps on the underlying Tully Limestone (Taghanic Onlap) and was deposited in shallow water, far removed from clastic dilution (Smith et al. 2019). **a** A hand specimen from Fall Brook (near Geneseo, NY), the type section of the Geneseo Shale. The specimen shows pyritic streaks mostly in the lower half (yellow arrows), and was collected from directly above the Tully Limestone (Fig. 16). **b** A drill core sample of Geneseo shale with abundant pyritic streaks (yellow arrows)

show that most pyrite forms in the uppermost few centimeters of the sediment (Berner 1970; Canfield et al. 1992). In addition, studies of modern muds have also shown that the formation of framboidal pyrite formation is a consequence of greigite formation under mildly reducing conditions, and occurs at the redox interface that separates waters with dissolved oxygen from anoxic pore waters (Wilkin and Barnes 1997). Another requirement is that the pore waters be non-sulfidic (Berner 1981) so as to enable migration of dissolved iron to the redox interface. Pyrite framboids are the earliest precipitates in the polygon pyrite accumulations (Fig. 11c), and thus suggest an intimate association between redox the interface and polygon tunnels. Occurrence of marcasite (Fig. 11d) within Fe-sulfide accumulations that constitute the polygons also points to a situation where oxygen-bearing waters were interacting with previously formed pyrite (Schieber 2011b). Given that this juxtaposition of oxygen-bearing and anoxic waters occurred within a strongly reducing organic-rich sediment, and that the redox interface was geometrically guided by an underlying structure of polygonal shape, we can make some fundamental conclusions about the nature of the polygons. The polygons were filled with oxygen-bearing waters, they were surrounded by anoxic non-sulfidic waters, and thus the only plausible source of oxygen is from the overlying bottom waters, a few millimeters to centimeters above. So, paradoxically, the presence of pyritic polygons has fundamental implications with respect to their very nature and the oxygenation state of the water overlying these organic-rich sediments.

In modern sediments, oxygen either is introduced to the near-surface sediment via burrows and the ventilating activity of infauna (Bromley 1996) or by downward diffusion from overlying waters. The latter, however, is an unlikely oxygen source for the polygons because downward diffusing oxygen it would have been consumed by aerobic respiration (Burdige 2006) in the organic-rich substrate. So, for the sake of precipitating the pyrite in the geometry we find it in, the polygon forming redox interface must have been an open tube system that was physically connected to overlying oxygen-bearing waters. Structures of that kind are known from the modern seafloor. They have been described as graphoglyptid burrows (Ekdale 1980) that consist of patches of polygonal tunnel systems that are connected by shafts to the overlying seawater.

In the case of the black shales examined for this study, the trace-makers may have been several millimeters across (Fig. 12) and of vermiform morphology. Thus, they probably were soft bodied macrobenthos and probably were ecologically capable of surviving dysoxic bottom water conditions to thrive. Observing that in both the New Albany and the Bakken Shale, the polygon-bearing intervals alternate with more conventional macrobioturbated strata (Figs. 10, 13) opens the distinct possibility that the latter may represent moderately dysoxic conditions, whereas the polygons

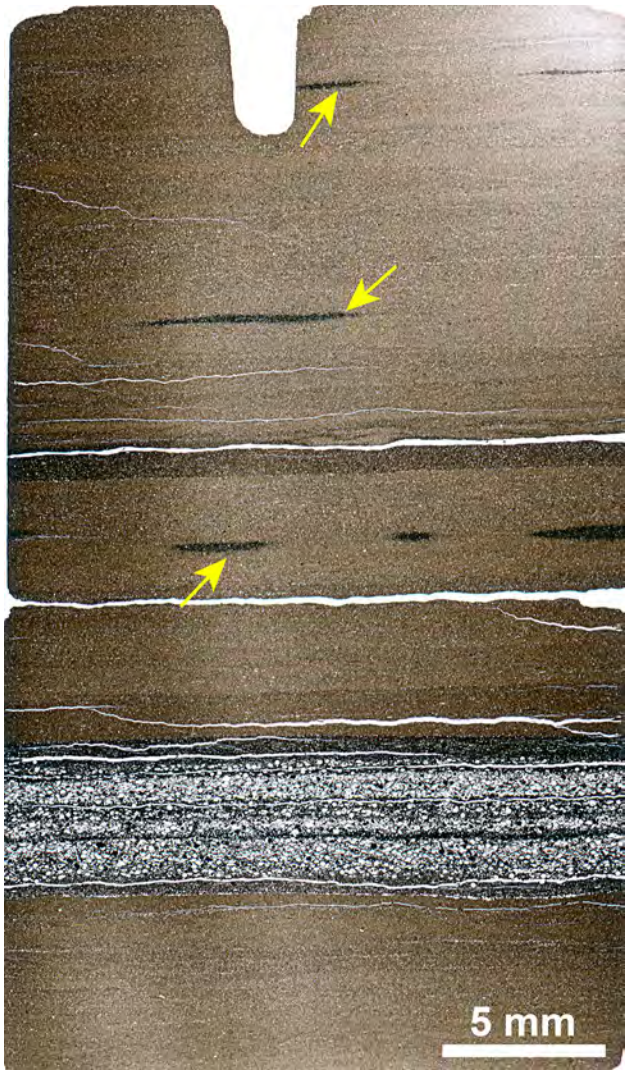

Fig. 15 Detail view of the lowermost Geneseo. It is a black shale with well-developed pyritic streaks (yellow arrows) that occur in three discrete horizons and very much resemble those seen in the New Albany (Fig. 5) and Bakken shales

represent severely dysoxic conditions that excluded other macrofauna from disturbing the sediment (Tyson and Pearson 1991).

Additional support for a worm-like creature occupying these tunnels comes from the observation of widely spaced mineral inclusions in the pyrite that constitutes the polygons (Fig. 11a), a feature not observed outside of the polygons (Fig. 11b). A texture like shown in Fig. 11a requires some kind of support medium for the mineral grains to stay in place (and separated) and allow pyrite growth between them. The slime secreted by worms traversing the sediment has been identified as a likely cause for this texture (Schieber 2002). Worms that pass through unconsolidated sediment produce mucus to ease their passage and leave behind a slime trail (Bromley 1996), and may also use mucus secretions to stabilize burrow walls in water-rich substrates (Thomsen and Vorren 1984). The wall-forming mucus is comparable in many respects to agar, a widely used culture medium in microbiology (Stanier et al. 1986).

On the basis of petrographic and geochemical considerations, and in combination with the overall geometry of the pyrite accumulations, a biogenic origin for the polygon horizons seems most plausible. The causing organism may have been a worm-like creature that stabilized its tunnels with mucus secretions and kept the structure connected to the overlying water body. The wall stabilizing mucus secretions may also have provided a preferred growth substrate for microbes, including the sulfate reducers that produced the pyrite. Graphoglyptid burrows as described by Ekdale (1980) appear to be a rather fitting modern analog.

Paleoenvironmental and paleoecological significance

Graphoglyptids are delicate, shallow tiered open structures produced in stagnant and resource-limited environments, and most of the examples in the literature are reported from deep-sea flysch environments that are grouped in the Nereites ichnofacies (Seilacher 2007). A few recent studies, however, have found evidence of their occurrence in shallow marine environments (e.g., tidal flat, prodelta, mid-to-deep shelf; Minter et al. 2006; Fürsich et al. 2007; Metz 2012). In both settings the dominant preservation is epirelief, due to distal turbidites or tempestites that eroded into the substrate and cast the burrows with sand (Crimes 1973; Fürsich et al. 2007). Due to the organic-rich sediment and the oxygen requirements of the trace maker, the graphoglyptids identified in this study most likely were constructed close to the sediment–water interface, not unlike the modern examples described by Ekdale (1980). Water content in the top centimeters of marine muds at the time of deposition can be as high as 90% by volume, and such muds are commonly referred to as soupgrounds (Bromley 1996; Dashtgard et al. 2015). Soupground dwellers either secrete a burrow lining to maintain an open burrow, or swim through the sediment and leave behind soft-sediment deformational structures such as mantle and swirl structures (Bromley 1996; Lobza and Schieber 1999).

On the basis of above considerations, it was presumed in previous studies that graphoglyptids should possess a burrow lining (Seilacher 2007; Lehane and Ekdale 2013). Although graphoglyptids share morphological traits with grazing traces such as *Cosmorhaphe* or *Helminthoraphe*, Seilacher (1977) recognized that some are too complicated to be rationalized as grazing traces and more likely function as a location to culture microbes or meiofauna for food within a mucus-based burrow lining. Ekdale et al. (1984) defined "agrichnia" as a new ethological category

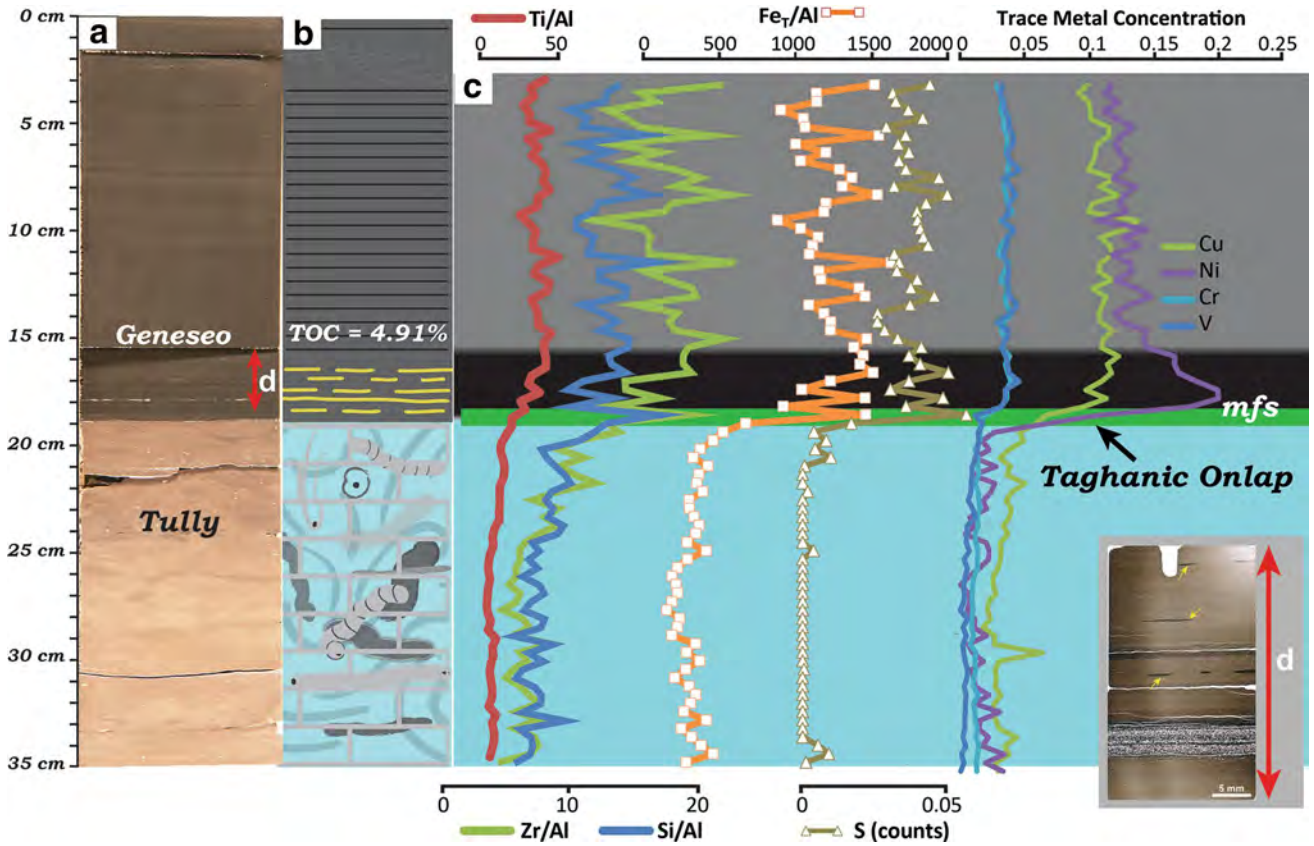

Fig. 16 **a** Drill core from the Tully–Geneseo contact. **b** A lithologic summary that shows the pyritic streak black shale directly above the base of the Geneseo (yellow lined pattern). **c** X-ray fluorescence data and derived detrital (Ti/Al, Si/Al, Zr/Al) and redox proxies (Fe/Al, V/Cr) that highlight the distal and condensed nature of the basal Geneseo. **d** The location of the thin section shown in Fig. 15

to describe this suite of traces. Fractal analysis on selected trace fossils showed that graphoglyptids have a lower fractal dimension than pascichnia and fodinichnia traces (Lehane and Ekdale 2013), suggesting that graphoglyptids do not signify an optimal foraging strategy such as grazing or mining, but instead represent agricultural behaviors. A modern analog to graphoglyptids, belonging to the ichnogenus *Paleodictyon*, has been found in deep-sea sediments, but staining techniques to identify a mucus lining were unsuccessful (Rona et al. 2009). Currently, no mucus linings have been identified in fossil examples by either textural or geochemical methods (Lehane and Ekdale 2013). At present, floating detrital mineral grains in polygon forming pyrite (Fig. 11a) of the New Albany Shale are the only documentation of likely mucus linings in graphoglyptid burrows. The importance of mucus linings as sites of diagenetic mineral precipitation has been pointed out by multiple authors (Canfield et al. 1998; Donald and Southam 1999; Grimes et al. 2001; Schieber 2002).

The Bakken, New Albany, and (presumed) Geneseo graphoglyptids are associated with dysoxic facies trace fossils such as *Zoophycos* and allied ichnogenera (Schieber and Lazar 2004; Lazar 2007; Wilson and Schieber 2015). The presence of abundant lags, scours, ripples and laterally extensive erosion surfaces indicates that deposition of these shale intervals took place in shallow waters (< 50 m) commonly disturbed by storms and currents (Schieber 1994, 1998; Schieber and Lazar 2004; Lazar 2007; Wilson and Schieber 2015). Because in modern environments, analog graphoglyptids occur a few millimeters below the sediment–water interface (Ekdale 1980), the preservation of these traces in Devonian black shales might suggest that intermittent erosion was minimal when the pyrite-streaked shales were deposited.

Given the similarity of lithofacies that host graphoglyptids in the Bakken, Geneseo, and New Albany Shale intervals (Figs. 4, 9, 12, 14), very similar depositional environments are indicated. Envisioned controls on graphoglyptid formation in these shales are: (1) very small sedimentation rates, (2) the type of organic matter within the sediment, and (3) oxygen concentrations within pore spaces. Evidence for small sedimentation rates is provided by algal cysts (Tasmanites) that are partially or completely filled with diagenetic minerals (pyrite or chalcedony; Schieber 1996; Schieber and Baird 2001; Mastalerz et al. 2013). Unless sedimentation rates were very small, these cysts should

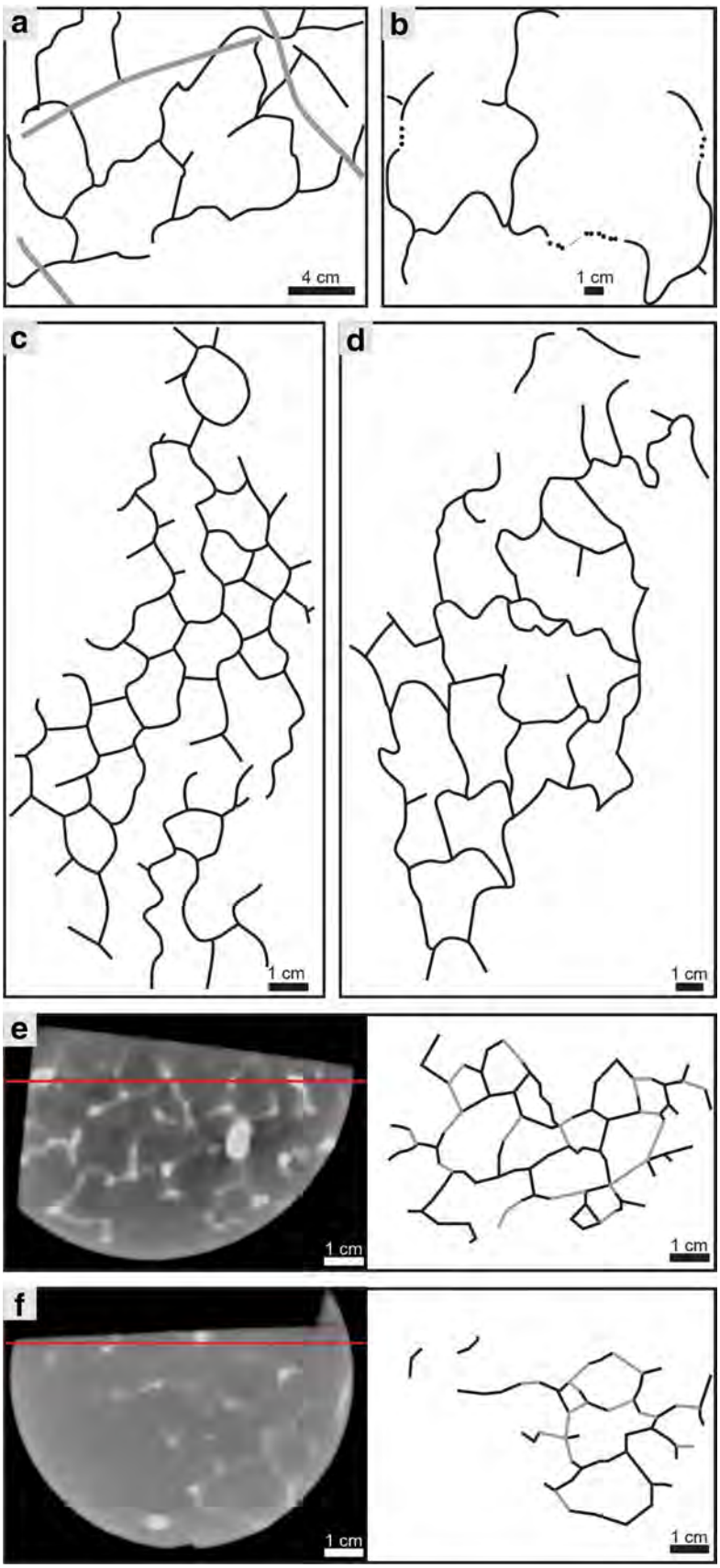

Fig. 17 Schematic drawings of graphoglyptids and New Albany Shale polygonal structures. **a** *Megagrapton*. Modified from Lehane and Ekdale (2013). **b**, **c** *Megagrapton irregulare*. Modified from Seilacher (1977). **d** *Megagrapton aequale*. Modified from Seilacher (1977). **e**, **f** Pictures and line sketches of polygonal structures from the New Albany Shale. Black lines mark readily identified pyrite concentrations, gray lines mark more subtle to barely visible pyrite concentrations

have been compacted early in depositional history (Schieber 1998). Algal cysts are abundantly observed in SEM (Fig. 14) and align with average $\delta^{13}C$ values of Devonian shales that point to dominant marine-derived organic matter in the studied intervals (Maynard 1981; Wilson and Schieber 2017).

Conclusions

The reported occurrences of graphoglyptids in Devonian Shales of North America are the first graphoglyptids described from these successions. Whereas all previous reports of graphoglyptids describe them as preserved in positive hyporelief on the underside of sandstone beds, the occurrences described here are the first documentation of graphoglyptids in full relief preservation within a mudstone matrix. They are also the first report of graphoglyptids in organic-rich black shales. In the latter context, they provide further evidence that accumulation of laminated black shales can indeed occur in absence of anoxic bottom waters. Interestingly, even though pyrite in black shales still carries an (undeserved) connotation of "anoxic", consideration of pyrite petrography and distribution actually provides the rationale for making the host shales "non-anoxic" black shales. The floating detrital mineral grains in polygon forming pyrite constitute the first documentation of likely mucus linings in graphoglyptid burrows.

An essential tool for graphoglyptids detection were CT scans of segments of cores. The observed graphoglyptids consist of irregular polygonal structures and are very similar to the ichnogenus *Megagrapton* (Fig. 17). On slabbed core, graphoglyptid traces appear as discontinuous, parallel, pyritic streaks. These can easily be misidentified as pyritized silt laminae, but nonetheless hold promise to alert us to the potential presence of polygonal structures and graphoglyptids within the rock volume. If thin section examination indicates in a given rock that pyritic streaks are mostly pyrite and not silt associated, to examine the rock via CT scan for potential graphoglyptid traces should be the next step. Also, if pyrite-streaked black shales alternate with less carbonaceous macro-burrowed horizons, it may indicate that the black shale intervals were deposited under oxygenation conditions favorable for graphoglyptid trace-makers.

The identification of graphoglyptids in this study suggests that other Phanerozoic black shale formations should be re-evaluated to determine if these traces existed elsewhere. If indeed black shale successions from other time intervals and locations show this feature to be widespread, it would significantly impact our understanding of ocean oxygenation through geologic time.

Acknowledgements We recognize the sponsors of the Indiana University Shale Research Consortium which provided student support. We are grateful for the reviews provided by Germán Otharán and an anonymous reviewer, as well as the support from Editor-in-Chief Mike Reich. Various student research grants were provided by GSA, SEPM, and AAPG (Pittsburgh Association of Petroleum Geologists Named Grant, Richard W. Beardsley Named Grant) which supported field and analytical work. A National Science Foundation equipment grant to J. Schieber (EAR-0318769) provided funds for the purchase of the analytical SEM that was used to acquire SEM images for this article.

References

Algeo, T.J., T.W. Lyons, R.C. Blakey, and D.J. Over. 2007. Hydrographic conditions of the Devono-Carboniferous North American Seaway inferred from sedimentary Mo-TOC relationships. *Palaeogeography, Palaeoclimatology, Palaeoecology* 256: 204–230.

Bednarz, M., and D. McIlroy. 2012. Effect of phycosiphoniform burrows on shale hydrocarbon reservoir quality. *AAPG Bulletin* 96: 1957–1980.

Berner, R.A. 1970. Sedimentary pyrite formation. *American Journal of Science* 2: 1–23.

Berner, R.A. 1981. A new geochemical classification of sedimentary environments. *Journal Sedimentary Petrology* 51: 359–365.

Berner, R.A. 1990. Atmospheric carbon dioxide levels over Phanerozoic time. *Science* 249: 1382–1386.

Boyer, D.L., and M.L. Droser. 2011. A combined trace- and body-fossil approach reveals high-resolution record of oxygen fluctuations in Devonian seas. *Palaios* 26: 500–508.

Brett, C.E., and P.A. Allison. 1998. Paleontological approaches to the environmental interpretation of marine mudrocks. In *Shales and mudstones I*, eds. J. Schieber, W. Zimmerle, and P. Sethi, 301–349. Stuttgart: Schweizerbart.

Bromley, R.G. 1996. *Trace fossils: biology, taphonomy and applications*. London: Chapman and Hall.

Burdige, D. 2006. *Geochemistry of marine sediments*. Princeton: Princeton University.

Buschbach, T.C., and D.R. Kolata. 1990. Regional setting of Illinois Basin. In *Interior Cratonic Basins*, eds. M.W. Leighton, D.R. Kolata, D.F. Oltz, and J.J. Eidel. *AAPG Memoir* 51: 29–55.

Canfield, D.E., R. Raiswell, and S. Bottrell. 1992. The reactivity of sedimentary iron toward sulfide. *American Journal of Science* 292: 659–683.

Canfield, D.E., B.P. Boudreau, A. Mucci, and J.K. Gundersen. 1998. The early diagenetic formation of organic sulfur in the sediments of Mangrove Lake, Bermuda. *Geochimica et Cosmochimica Acta* 62: 767–781.

Crimes, T.P. 1973. From limestones to distal turbidites: a facies and trace fossil analysis in the Zumaya flysch (Paleocene-Eocene), North Spain. *Sedimentology* 20: 105–131.

Cullen, D.J. 1973. Bioturbation of superficial marine sediments by interstitial meiobenthos. *Nature* 242: 323–324.

Cuomo, M.C., and P.R. Bartholomew. 1991. Pelletal black shale fabrics: their origin and significance. In *Modern and ancient continental shelf anoxia*, eds. R.V. Tyson and T.H. Pearson. *Geological Society of London, Special Publication* 58: 221–232.

Cuomo, M.C., and D.C. Rhoads. 1987. Biogenic sedimentary fabrics associated with pioneering polychaete assemblages: modern and ancient. *Journal of Sedimentary Petrology* 57: 537–543.

Dashtgard, S.E., J.W. Snedden, and J.A. MacEachern. 2015. Unbioturbated sediments on a muddy shelf: Hypoxia or simply reduced oxygen saturation? *Palaeogeography, Palaeoclimatology, Palaeoecology* 425: 128–138.

De Witt, W., and G.W. Colton. 1978. Physical stratigraphy of the Genesee formation (Devonian) in western and central New York. *U.S. Geological Survey* 1032-A: 1–22.

Donald, R., and G. Southam. 1999. Low temperature anaerobic bacterial diagenesis of ferrous monosulfide to pyrite. *Geochemica et Cosmochimica Acta* 63: 2019–2023.

Ekdale, A.A. 1980. Graphoglyptid burrows in modern deep-sea sediment. *Science* 207: 304–306.

Ekdale, A.A., and T.R. Mason. 1988. Characteristic trace-fossil associations in oxygen-poor sedimentary environments. *Geology* 16: 720–723.

Ekdale, A.A., R.G. Bromely, and S.G. Pemberton. 1984. Ichnology: the use of trace fossils in sedimentology and stratigraphy. *SEPM Short Course* 15: 1–317.

Ettensohn, F.R., M.L. Miller, S.B. Dillman, T.D. Elam, K.L. Geller, D.R. Swager, G. Markowitz, R.D. Woock, and L.S. Barron. 1988. Characterization and implications of the Devonian-Mississippian black shale sequence, eastern and central Kentucky, U.S.A.: pycnoclines, transgression, regression, and tectonism. *Canadian Society of Petroleum Geologists Memoir* 14: 323–345.

Faill, R.T. 1985. The Acadian orogeny and the Catskill Delta. In *The Catskill Delta*, eds. D.L. Woodrow and W.D. Sevon. *Geological Society of America, Special Paper* 201: 15–37.

Fischer, A.G. 1981. Climatic oscillations in the biosphere. In *Biotic crises in ecological and evolutionary time*, ed. M. Nitecki, 103–131. New York: Academic Press.

Fürsich, F.T., J. Taheri, and M. Wilmsen. 2007. New occurrences of the trace fossil *Paleodictyon* in shallow marine environments: examples from the Triassic–Jurassic of Iran. *Palaios* 22: 408–416.

Grimes, S.T., F. Brock, D. Rickard, K.L. Davies, D. Edwards, D.E.G. Briggs, and R.J. Parkes. 2001. Understanding fossilization: experimental pyritization of plants. *Geology* 29: 123–126.

Hallam, A., and P.B. Wignall. 1997. *Mass Extinctions and Their Aftermath*. Oxford: Oxford University Press.

House, M.R. 2002. Strength, timing, setting and cause of Mid-Palaeozoic extinctions. *Palaeogeography, Palaeoclimatology, Palaeoecology* 181: 5–25.

Jordan, D.W. 1985. Trace fossils and depositional environments of Upper Devonian black shales, east-central Kentucky, USA. In *Biogenic structures: their use in interpreting depositional environments*, ed. H.A. Currany. *SEPM Special Publication* 35: 279–298.

Ketcham, R.A., and W.D. Carlson. 2001. Acquisition, optimization and interpretation of X-ray computed tomographic imagery: applications to the geosciences. *Computers and Geosciences* 27: 381–400.

Kolata, D.R., and W.J. Nelson. 1990. Tectonic history of the Illinois Basin. In *Interior Cratonic Basins*, eds. M.W. Leighton, D.R. Kolata, D.F. Oltz, and J.J. Eidel. *AAPG Memoir* 51: 263–285.

Lazar, O.R. 2007. *Redefinition of the New Albany Shale of the Illinois Basin: an integrated, stratigraphic, sedimentologic, and geochemical study*, 1–363. Dissertation, Indiana University, Bloomington, Ind.

Lazar, R., K.M. Bohacs, J. Schieber, J. Macquaker, and T. Demko. 2015a. Mudstone primer: lithofacies variations, diagnostic criteria, and sedimentologic/stratigraphic implications at the lamina to bedset scale. *SEPM Concepts in Sedimentology and Paleontology* 12: 1–198.

Lazar, O.R., K.M. Bohacs, J.H.S. Macquaker, J. Schieber, and T.M. Demko. 2015b. Integrated approach for the nomenclature and description of the spectrum of fine-grained sedimentary rocks. *Journal of Sedimentary Research* 85: 230–246.

Lehance, J.R., and A.A. Ekdale. 2013. Fractal analysis of graphoglyptid trace fossils. *Palaios* 28: 23–32.

Lineback, J.A. 1968. Subdivisions and depositional environments of New Albany Shale (Devonian-Mississippian) in Indiana. *American Association of Petroleum Geologists Bulletin* 52: 1291–1303.

Lineback, J.A. 1970. Stratigraphy of the New Albany Shale in Indiana. *Indiana Geological Survey, Bulletin* 44: 73.

Lobza, V., and J. Schieber. 1999. Biogenic sedimentary structures produced by worms in soupy, soft muds: observations from the Chattanooga Shale (Upper Devonian) and experiments. *Journal of Sedimentary Research* 69: 1041–1049.

Mastalerz, M., A. Schimmelmann, A. Drobniak, and Y.Y. Chen. 2013. Porosity of Devonian and Mississippian New Albany Shale across a maturation gradient: Insights from organic petrology, gas adsorption, and mercury intrusion. *AAPG Bulletin* 97: 1621–1643.

Maynard, J.B. 1981. Carbon isotopes as indicators of dispersal patterns in Devonian–Mississippian shales of the Appalachian Basin. *Geology* 9: 262–265.

McGhee, G.R., Jr. 1996. *The late Devonian mass extinction*. New York: Columbia University Press.

Mees, F., R. Swennen, M. Van Geet, and P. Jacobs. 2003. Applications of X-ray computed tomography in the geosciences. *Geological Society of London* 215: 1–6.

Metz, R. 2012. The trace fossil *Paleodictyon* within the *Cruziana* ichnofacies: first record from the Devonian in Pennsylvania. *Ichnos* 181: 190–193.

Minter, N.J., L.A. Buatois, S.G. Lucas, S.J. Braddy, and J.A. Smith. 2006. Spiralshaped graphoglyptids from an early Permian intertidal flat. *Geology* 34: 1057–1060.

Montgomery, S.L. 1996. Mississippian Lodgepole play, Williston Basin: a review. *AAPG Bulletin* 80: 795–810.

O'Brien, N.R., and R.M. Slatt. 1990. *Argillaceous rock atlas*. New York: Springer

Pike, J., J.M. Bernhard, S.G. Moreton, and I.B. Butler. 2001. Microbioirrigation of marine sediments in dysoxic environments: Implications for early sediment fabric formation and diagenetic processes. *Geology* 29: 923–926.

Raiswell, R., and D.E. Canfield. 1998. Sources of iron for pyrite formationin marine sediments. *American Journal of Science* 298: 219–245.

Rona, P.E., A. Seilacher, C.D. Vargas, A.J. Gooday, J.M. Bernhard, S. Bowser, C. Vetriani, C.O. Wirsen, L. Mullineaux, R. Sherrell, J.F. Grassle, S. Low, and R.A. Lutz. 2009. *Paleodictyon nodosum*: a living fossil on the deep-sea floor. *Deep-Sea Research II* 56: 1700–1712.

Sageman, B.B., A.E. Murphy, J.P. Werne, C.A. Ver Straeten, D.J. Hollander, and T.W. Lyons. 2003. A tale of shales: the relative roles of production, decomposition, and dilution in the accumulation of organic-rich strata, Middle-Upper Devonian, Appalachian Basin. *Chemical Geology* 195: 229–273.

Savrda, C.E., and D.J. Bottjer. 1989. Anatomy and implications of bioturbated beds in "black shale" sequences: examples from the Jurassic Posidonienschiefer (Southern Germany). *PALAIOS* 4: 330–342.

Savrda, C.E., and D.J. Bottjer. 1991. Oxygen-related biofacies in marine strata: an overview and update. In *Modern and ancient continental shelf anoxia*, eds. R.V. Tyson and T.H. Pearson. *Geological Society of London, Special Publications* 58: 201–219.

Savrda, C.E., and K. Ozalas. 1993. Preservation of mixed-layer ichnofabrics in oxygenation-event beds. *PALAIOS* 8: 609–613.

Savrda, C.E., D.J. Bottjer, and D.S. Gorsline. 1984. Development of a comprehensive oxygen-deficient marine biofacies model: evidence from Santa Monica, San Pedro, and Santa Barbara Basins, California continental borderland. *AAPG Bulletin* 68: 1179–1192.

Schieber, J. 1994. Evidence for episodic high energy events and shallow water deposition in the Chattanooga Shale, Devonian, central Tennessee, U.S.A. *Sedimentary Geology* 93: 193–208.

Schieber, J. 1996. Early diagenetic silica deposition in algal cysts and spores; a source of sand in black shales? *Journal of Sedimentary Research* 66: 175–183.

Schieber, J. 1998. Sedimentary features indicating erosion, condensation, and hiatuses in the Chattanooga Shale of Central Tennessee: relevance for sedimentary and stratigraphic evolution. In *Shales and mudstones I*, eds. J. Schieber, W. Zimmerle, and P. Sethi, 187–215. Stuttgart: Schweizerbart.

Schieber, J. 2002. The role of an organic slime matrix in the formation of pyritized burrow trails and pyrite concretions. *PALAIOS* 17: 104–109.

Schieber, J. 2003. Simple gifts and buried treasures–implications of finding bioturbation and erosion surfaces in black shales. *The Sedimentary Record* 1: 4–8.

Schieber, J. 2011a. Reverse engineering mother nature—shale sedimentology from an experimental perspective. *Sedimentary Geology* 238: 1–22.

Schieber, J. 2011b. Marcasite in black shales—a mineral proxy for oxygenated bottom waters and intermittent oxidation of Carbonaceous Muds. *Journal of Sedimentary Research* 81: 447–458.

Schieber, J. 2013. SEM observations on ion-milled samples of Devonian Black Shales from Indiana and New York: the petrographic context of multiple pore types. *AAPG Memoir* 102: 153–172.

Schieber, J., and G. Baird. 2001. On the origin and significance of pyrite spheres in Devonian black shales of North America. *Journal of Sedimentary Research* 71: 155–166.

Schieber, J., and R.O. Lazar. 2004. Devonian black shales of the eastern U.S.: new insights into sedimentology and stratigraphy from the subsurface and outcrops in the Illinois and Appalachian Basins. Field guide for the 2004 Great Lakes Section SEPM Annual Field Conference. *Indiana Geological Survey Open File Study* 4–5: 1–90.

Schieber, J., and R.D. Wilson. 2021. Burrows without a trace – How meioturbation affects rock fabrics and leaves a record of meiobenthos activity in shales and mudstones. *PalZ. Paläontologische Zeitschrift*. https://doi.org/10.1007/s12542-021-00590-7.

Schieber, J., R. Lazar, K. Bohacs, B. Klimentidis, J. Ottmann, and M. Dumitrescu. 2016. An SEM study of porosity in the eagle ford shale of Texas—pore types and porosity distribution in a depositional and sequence stratigraphic context. *AAPG Memoir* 110: 153–172.

Schieber, J., X. Shao, Z. Yawar, and B. Liu. 2021. Cryptic burrow traces in black shales—a petrographic Rorschach test or the real thing? *Sedimentology* 68: 2707.

Scotese, C.R. 2014. *Atlas of Devonian paleogeographic maps, PALEOMAP atlas for ArcGIS, the late Paleozoic, maps 65–72, Mollweide projection*, vol. 4. Evanston: PALEOMAP Project.

Scotese, C.R., and W.S. McKerrow. 1990. Revised world maps and introduction. In *Palaeozoic palaeogeography and biogeography*, eds. W.S. McKerrow and C.R. Scotese. *Geological Society of London, Memoir* 12: 1–21.

Seilacher, A. 1977. Pattern analysis of Paleodictyon and related trace fossils. In *Trace Fossils 2*, eds. T.P. Crimes, and J.C. Harper. *Geological Journal, Special Issue* 9: 289–334.

Seilacher, A. 2007. *Trace fossil analysis*. Berlin: Springer.

Sepkoski, J.J., and D.M. Raup. 1986. Periodicity in marine extinction events. In *Dynamics of extinctions*, ed. D.K. Elliot, 3–36. New York: Wiley.

Smith, L.B., J. Schieber, and R.D. Wilson. 2019. Shallow-water onlap model for the deposition of Devonian black shales in New York, USA. *Geology* 47: 279–283.

Stanier, R.Y., J.L. Ingraham, M.L. Wheeiis, and P.R. Painter. 1986. *The microbial world*. Englewood Cliffs: Prentice-Hall.

Thomsen, E., and T.O. Vorren. 1984. Pyritization of tubes and burrows from Late Pleistocene continental shelf sediments off North Norway. *Sedimentology* 31: 481–492.

Trabucho-Alexandre, J., R. Dirkx, H. Veld, G. Klaver, and P. de Boer. 2012. Toarcian black shales in the Dutch Central Graben: Record of energetic, variable depositional conditions during an Oceanic Anoxic Event. *Journal of Sedimentary Research* 82: 104–120.

Tyson, R.V., and T.H. Pearson. 1991. Modern and ancient continental shelf anoxia: an overview. In *Modern and ancient continentalshelf anoxia*, eds. R.V. Tyson, and T.H. Pearson. *Geological Society of London, Special Publications* 58, 1–24.

Werne, J.P., B.B. Sageman, T.W. Lyons, and D.J. Hollander. 2002. An integrated assessment of a "type euxinic" deposit: evidence for multiple controls on black shale deposition in the middle Devonian Oatka Creek formation. *American Journal of Science* 302: 110–143.

Wetzel, A. 2010. Deep-sea ichnology: observations in modern sediments to interpret fossil counterparts. *Acta Geologica Polonica* 60: 125–138.

Wilkin, R.T., and H.L. Barnes. 1997. Formation processes of framboidal pyrite. *Geochimica et Cosmochimica Acta* 60: 323–339.

Wilson, R.D., and J. Schieber. 2015. Sedimentary facies and depositional environment of the Middle Devonian geneseo formation of New York, U.S.A. *Journal of Sedimentary Research* 85: 1393–1415.

Wilson, R.D., and J. Schieber. 2016. The influence of primary and secondary sedimentary features on reservoir quality: examples from the Geneseo formation of New York, U.S.A. In *Imaging unconventional reservoir pore systems*, ed. T. Olson. *AAPG Memoir* 112: 167–184.

Wilson, R.D., and J. Schieber. 2017. Sediment transport processes and lateral facies gradients across a muddy shelf: examples from the Geneseo formation of central New York, United States. *AAPG Bulletin* 101: 423–431.

Wilson, R.D., J. Chitale, P. Montgomery, K. Huffman, and S. Prochnow. 2020. Evaluating the depositional environment, lithofacies variation, and diagenetic processes in the Wolfcamp B and Spraberry intervals in the Midland Basin: implications for reservoir quality and distribution. *AAPG Bulletin* 104: 1287–1321.

Witzke, B.J., and P.H. Heckel. 1988. Paleoclimatic indicators and inferred Devonian paleolatitudes of Euramerica. In *Devonian of the world*, eds. N.J. McMillan, A.F. Embry, and D.J. Glass. *Canadian Society of Petroleum Geologists, Memoir* 14: 49–63.

Woodrow, D.L. 1985. Paleogeography, paleoclimate, and sedimentary processes of the Late Devonian Catskill Delta. In *The Catskill Delta*, eds. D.L. Woodrow and W.D. Sevon. *Geological Society of America, Special Paper* 201: 51–63.